1996

Heat shock factor gains access to the yeast HSC82 promoter independently of other sequence-specific factors and antagonizes nucleosomal repression of basal and induced transcription

Alexander M. Erkine
Butler University, aerkine@butler.edu

C. C. Adams

T. Diken

D. S. Gross

MOLECULAR AND CELLULAR BIOLOGY, Dec. 1996, p. 7004–7017 Vol. 16, No. 12
0270-7306/96/$04.00+0

Heat Shock Factor Gains Access to the Yeast *HSC82* Promoter Independently of Other Sequence-Specific Factors and Antagonizes Nucleosomal Repression of Basal and Induced Transcription

ALEXANDER M. ERKINE, CHRISTOPHER C. ADAMS, TUBA DIKEN, AND DAVID S. GROSS*

Department of Biochemistry and Molecular Biology, Louisiana State University Medical Center, Shreveport, Louisiana 71130

Received 7 February 1996/Returned for modification 19 July 1996/Accepted 26 August 1996

Transcription in eukaryotic cells occurs in the context of chromatin. Binding of sequence-specific regulatory factors must contend with the presence of nucleosomes for establishment of a committed preinitiation complex. Here we demonstrate that the high-affinity binding site for heat shock transcription factor (HSF) is occupied independently of other *cis*-regulatory elements and is critically required for preventing nucleosomal assembly over the yeast *HSC82* core promoter under both noninducing (basal) and inducing conditions. Chromosomal mutation of this sequence, termed HSE1, erases the HSF footprint and abolishes both transcription and in vivo occupancy of the TATA box. Moreover, it dramatically reduces promoter chromatin accessibility to DNase I and *Taq*I, as the nuclease-hypersensitive region is replaced by a localized nucleosome. By comparison, in situ mutagenesis of two other promoter elements engaged in stable protein-DNA interactions in vivo, the GRF2/REB1 site and the TATA box, despite reducing transcription three- to fivefold, does not compromise the nucleosome-free state of the promoter. The GRF2-binding factor appears to facilitate the binding of proteins to both HSE1 and TATA, as these sequences, while still occupied, are less protected from in vivo dimethyl sulfate methylation in a ΔGRF2 strain. Finally, deletion of a consensus upstream repressor sequence (URS1), positioned immediately upstream of the GRF2-HSE1 region and only weakly occupied in chromatin, has no expression phenotype, even under meiotic conditions. However, deletion of URS1, like mutation of GRF2, shifts the translational setting of an upstream nucleosomal array flanking the promoter region. Taken together, our results argue that HSF, independent of and dominant among sequence-specific factors binding to the *HSC82* upstream region, antagonizes nucleosomal repression and creates an accessible chromatin structure conducive to preinitiation complex assembly and transcriptional activation.

The promoter regions of eukaryotic genes consist of multiple *cis*-acting elements that serve as binding sites for regulatory proteins. Two categories of *cis*-regulatory sequences have been described. The general downstream elements, exemplified by the TATA box and initiator element, specify transcription start site selection (10), while specialized upstream elements, target sites for a variety of activators and repressors, regulate the rate of transcription initiation (66). Since these elements must function in the context of chromatin, both the sequence-specific upstream regulatory proteins and components of the general transcriptional machinery must overcome the potential steric hindrance imposed by nucleosomes during the recognition of, and subsequent association with, a target promoter (reviewed in references 21, 27, 35, 71, and 72). Indeed, compaction of promoter DNA into nucleosomes prevents the initiation of transcription, both in vitro and in vivo (24, 34, 43, 62, 73). Therefore, *cis*-regulatory elements of transcriptionally poised genes usually reside within regions of chromatin that are hypersensitive to DNase I and, by inference, free of canonical nucleosomes (14, 26).

DNase I-hypersensitive regions provide "open windows" through which transcription factors and RNA polymerase holoenzyme gain access to the template DNA. What are the biochemical determinants of such accessible chromatin structures? The TATA-binding basal transcription factor, TFIID, may fulfill this function under certain circumstances, for it effectively potentiates promoter function when preincubated with a naked DNA template either during in vitro chromatin reconstitution (7, 73) or following injection into fertilized *Xenopus* eggs (57). Nonetheless, when histones are added to naked DNA simultaneously with TFIID, nucleosomal repression can be prevented only if an upstream activator protein is also included (74). Indeed, specialized upstream factors appear to normally underlie the genesis of accessible, nucleosome-free (or disrupted) regions at native promoters and enhancers (18, 20, 24, 30, 44, 67). That this activity is central to the normal function of upstream activators is suggested by the fact that physiological levels of transcriptional induction in reconstituted systems is contingent upon prior assembly of template DNA into stable, uniformly spaced nucleosomes (38, 53). However, largely unknown is the interrelationship of upstream factors in the remodeling process. Can a single, dominant upstream activator prompt the formation of a nucleosome-free region within native chromatin, or is a nuclease-hypersensitive site the product of multiple sequence-specific factors? Such factors may outcompete histones at the replication fork to establish a nucleosome-free region (exclusion model); alternatively, they may bind and displace (or disrupt) a preexisting nucleosome (displacement model) (reviewed in reference 72). In the latter case, transcription factors may be assisted by ATP-dependent, multiprotein complexes such as SWI/SNF or NURF to reconfigure promoter chromatin structure (reviewed in references 31a and 55).

* Corresponding author. Phone: (318) 675-5027. Fax: (318) 675-5180. Electronic mail address: dgross@lsumc.edu.

TABLE 1. Yeast strains used

Yeast strain	Genotype	Reference
W303-1B	*MAT*α *ade2-1 can1-100 his3-11,15 leu2-3,112 trp1-1 ura3-1*	40
CUD82	*MAT***a** *ade2-1 can1-100 his3-11,15 leu2-3,112 trp1-1 ura3-1 hsc82*Δ*::URA3*	8
SLY101	*MAT*α *ade2-1 can1-100 his3-11,15 leu2-3,112 trp1-1 ura3-1 cyh2*^{r}	40
CRY102	SLY101; *hsc82*Δ*::CYH2*^{s}	This study
TAT100	CRY102; *hsc82*-ΔTATA	This study
TAT101	CRY102; *hsc82*-ΔTATA, ΔHSE1	This study
TAT102	CRY102; *hsc82*-ΔTATA, ΔHSE1, ΔURS1	This study
HSE100	W303-1B; *hsc82*-ΔHSE0	This study
HSE101	W303-1B; *hsc82*-ΔHSE1	This study
HSE102	W303-1B; *hsc82*-ΔHSE0, ΔHSE1	This study
GRF200	CRY102; *hsc82*-ΔGRF2	This study
URS100	CRY102; *hsc82*-ΔURS1	This study
URS101	CRY102; *hsc82*-ΔHSE0, ΔURS1	This study
URS102	CRY102; *hsc82*-ΔHSE1, ΔURS1	This study
URS103	CRY102; *hsc82*-ΔHSE0, ΔHSE1, ΔURS1	This study
WT-HSC	*MAT***a**/α *ade2-1 can1-100 his3-11,15 leu2-3,112 trp1-1 ura3-1 HSC82*$^+$ / *ade2-1 can1-100 his3-11,15 leu2-3,112 trp1-1 ura3-1 hsc82*Δ*::URA3*	This study
ΔURS1-HSC	*MAT***a**/α *ade2-1 can1-100 his3-11,15 leu2-3,112 trp1-1 ura3 cyh2*^{r} *hsc82-*Δ*URS1* / *ade2-1 can1-100 his3-11,15 leu2-3,112 trp1-1 ura3-1 hsc82*Δ*::URA3*	This study

We are interested in understanding the role of chromatin in the heat shock transcription mechanism. Stress-induced activation of heat shock genes from organisms as diverse as yeast, tomato, fly, and human is achieved by the binding of heat shock factor (HSF) to its target DNA sequences, heat shock elements (HSEs) (reviewed in reference 42). A notable difference between heat shock gene activation in the budding yeast *Saccharomyces cerevisiae* and higher eukaryotes is that *S. cerevisiae* HSF (ScHSF) is constitutively bound to high-affinity HSEs within chromatin, whereas metazoan HSF binds to DNA only following heat shock (25, 29, 60). This difference underlies the unique role of ScHSF in directing basal (nonactivated) transcription (48, 52) and in maintaining the promoter region of at least one heat shock gene, *HSP82*, in a DNase I-hypersensitive, nucleosome-free state (24).

Yeast *HSC82* is a constitutively expressed heat shock gene whose level of expression is enhanced severalfold following exposure to chemical or thermal stress (1, 8). That this induction occurs at the level of transcription is suggested by measurements of both its own transcript (1, 15) as well as that of *lacZ* in strains bearing an episomal *HSC82-lacZ* fusion gene (2). *HSC82* harbors a broad, heat-shock-invariant DNase I-hypersensitive domain localized to its 5′ end. Within this nucleosome-free zone are strong constitutive protein-DNA interactions that have been mapped at nucleotide resolution to the high-affinity HSE (HSE1), the consensus GRF2/REB1 site, and the TATA box (15). Here we investigate the structural and functional consequences of mutating these three sequences, as well as the promoter-proximal HSE (HSE0) and a consensus upstream repressor sequence (URS1). In situ mutagenesis of each of these five elements, individually and in combination, leads to the conclusion that the HSF-HSE1 complex not only plays a dominant role in remodeling promoter chromatin structure but can form independently of the other four sites. This observation provides a striking contrast to the *Drosophila hsp70* gene, where a specific in vivo architecture must be established by several independent factors to allow HSF access to the promoter (58).

MATERIALS AND METHODS

Yeast strains, cell growth, and heat shock. Strains of *S. cerevisiae* used in this study are listed in Table 1. Cells were grown in rich medium (1% yeast extract, 2% Bacto Peptone, 2% dextrose) to early log phase (~2×10^7 cells per ml; ~50 Klett units), heat shocked (30-to-39°C temperature upshift for 15 min), and metabolically poisoned with 20 mM sodium azide as previously described (25).

Sporulation. Diploid strains were preadapted to respiratory metabolism by growth in presporulation medium (1% potassium acetate, 0.67% yeast nitrogen base, 5% phthalic acid [pH 5.5] supplemented with the appropriate auxotrophic requirements). At a cell density of ~10^7/ml, cells were harvested by centrifugation, washed in sterile water, and resuspended in buffered sporulation medium (1% potassium acetate, 0.1% yeast extract [pH 7.0] supplemented with the appropriate auxotrophic requirements). Cultures were maintained at 30°C with vigorous shaking. Aliquots (10 ml) were removed at the appropriate times following the shift to sporulation medium, and total RNA was isolated and evaluated as previously described (1).

In vitro mutagenesis. Oligonucleotide-directed mutagenesis was performed on a *Bam*HI-*Kpn*I *HSC82* fragment (spanning −1341 to +321) cloned into M13mp18 as described previously (24). To disrupt HSE1, point mutations were introduced into each of the three conserved *n*GAA*n* units; a fourth point mutation was also introduced into the nonconserved GAA at −164. HSE0 was similarly disrupted by the introduction of four point mutations, while the GRF2 site was destroyed by a 6-bp substitution mutation. The HSE1 mutation destroys the −174 *Xba*I site, the HSE0 mutation creates a novel *Hae*III site at −134, and the GRF2 mutation creates a novel *Cla*I site at −205. Such sites permitted a convenient screen for transformants harboring the desired *hsc82* allele (see below). To disrupt the URS1 element at −226, the 11-bp region between −228 and −216 was deleted, while a 6-bp substitution mutation destroyed the TATA box at position −98. All five mutations (see Fig. 2) were confirmed by dideoxy sequencing of the appropriate M13 constructs.

Yeast strain construction. Strain W303-1B (*HSC82*$^+$) was used as the recipient for gene transplacement of *hsc82* alleles harboring mutations in either HSE0 or HSE1; the *hsc82*Δ*::CYH2*^{s} disruption strain, CRY102, was used as the recipient for construction of *hsc82* mutant strains bearing mutations in TATA, GRF2, or URS1 elements. In CRY102, an isogenic derivative of the *cyh2*^{r} strain SLY101 (40), the *HSC82 Bcl*I fragment, spanning −409 to +95, was replaced with a 1.6-kb *Pst*I fragment containing the *CYH2*^{s} gene, oriented codirectionally with *HSC82*. Inactivating mutations can be introduced into the *HSC82* gene due to the presence of *HSP82*; deletion of both *HSP90* genes is lethal (8). To permit two-step gene transplacement at the *HSC82* locus, the mutagenized *Bam*HI-*Kpn*I fragment was subcloned into pRS306, a *URA3*-containing yeast integrating vector (59). The resultant constructs were site directed to the *HSC82* locus by linearizing at the unique *Eco*RI site within *HSC82* at position −615. Selection on Ura$^-$ medium and counterselection on medium containing 1 mg of 5-fluoro-orotic acid per ml were done as previously described (40). In the case of transplacement in CRY102, loss of the host *hsc82*Δ*::CYH2*^{s} allele was initially screened by replica plating 5-fluoro-orotic acid-resistant clones onto rich medium containing cycloheximide.

In all cases, molecular verification of gene transplacement was achieved by Southern analysis; for selected alleles (*hsc82*-ΔHSE1, *hsc82*-ΔGRF2, and *hsc82*-ΔURS1), verification was extended to the nucleotide level by genomic sequencing. Gene transplacement was assayed by Southern analysis using probe C1 (Fig. 1B). In strains TAT100, TAT101, TAT102, URS100, URS101, URS102, and URS103, we confirmed that the 6.5-kb *Bam*HI fragment characteristic of the *hsc82*Δ*::CYH2*^{s} allele of strain CRY102 was replaced by a 5.4-kb *Bam*HI fragment (−1341 to +4100). In strains HSE101 and HSE102, the 1.06-kb *Xba*I fragment characteristic of the *HSC82*$^+$ allele (−1231 to −173) was replaced by

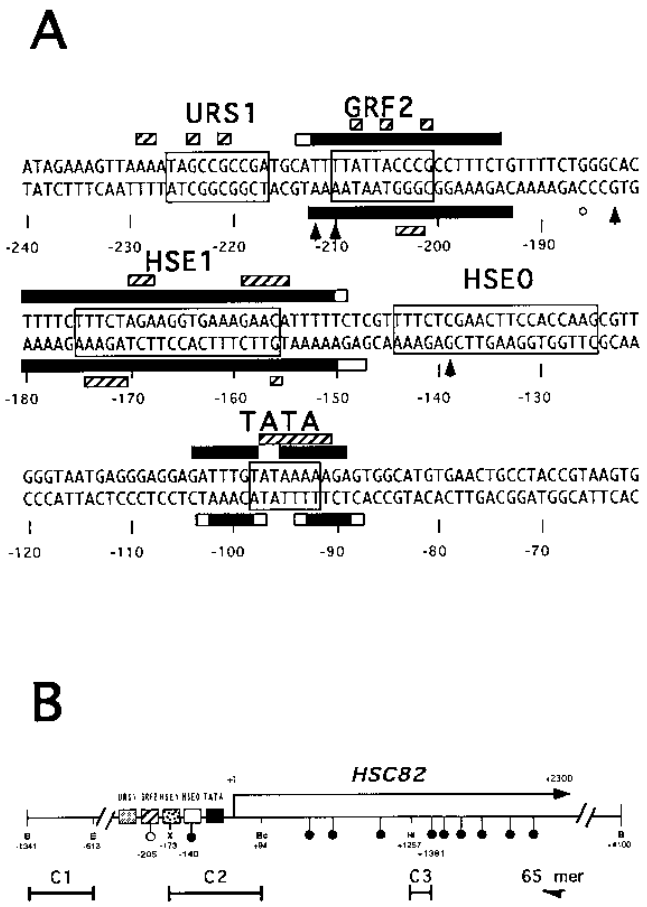

FIG. 1. *HSC82* upstream sequence, sites of DNase I protection in nuclei and DMS protection/hyperreactivity in intact cells, and a physical map of the chromosomal locus. (A) The upstream sequence of *HSC82*, numbered relative to the principal transcription initiation site (8). Sequences bearing homology to consensus regulatory elements in *S. cerevisiae* are boxed. The heat shock elements HSE0 and HSE1 each exhibit a 10/12 match to conserved nucleotides of the HSF consensus (consisting of tandem inverted repeats of *n*TTC*n*), while GRF2 and URS1 exhibit 8/8 and 10/10 matches to conserved nucleotides of their respective consensus sequences (17). Note that HSE1 exhibits a 13/16 match to a recent refinement of the *S. cerevisiae* HSF consensus (consisting of tandem inverted repeats of AGAAN [22]), whereas HSE0 exhibits only an 11/16 match, consistent with the observed occupancy of HSE1 but not HSE0 (Fig. 4 and 5). Nucleotides protected from DNase I are indicated by filled bars; uncertainty in the extent of DNase I protection is indicated by open bars. Nucleotides constitutively protected from DMS are indicated by striped bars, those constitutively hyperreactive to DMS are indicated by arrowheads, and a nucleotide exhibiting heat shock-inducible hyperreactivity is marked with an open circle. (Note that for the lower strand, DMS analysis extends from −212 to −120 only, while the upstream limit of DNase I analysis is to position −215.) Footprinting data are derived from this study (Fig. 4 and 5) and from reference 15. (B) Physical map of the *HSC82* locus on chromosome XIII. Locations of naturally occurring *Taq*I sites within the sequenced region (−1341 to +2257) are indicated by filled circles; a synthetic *Taq*I site, present only in the *hsc82*-ΔGRF2 allele, is indicated by an open circle. Locations of the four hybridization probes used in this study are also indicated. C1 to C3 represent RNA probes, synthesized in vitro as previously described (15). 65-mer, upper-strand-specific probe used to detect *HSC82* mRNA. B, *Bam*HI; E, *Eco*RI; X, *Xba*I; Bc, *Bcl*I; Hf, *Hin*fI.

a 6.5-kb *Xba*I fragment, while the 2.4-kb *Hae*III fragment characteristic of the *HSC82*$^+$ allele (−714 to +1686) was replaced by a 0.6-kb *Hae*III fragment in strains HSE100 and HSE102 (2).

The diploid strains WT-HSC and ΔURS1-HSC were constructed by mating the *MAT***a** *hsc82*Δ*::URA3* strain CUD82 (8) with either W303-1B (*MAT*α *HSC82*$^+$) or URS100 (*MAT*α *hsc82*Δ*-URS1*). These constructions were confirmed by Southern analysis and, in the case of ΔURS1-HSC, by genomic sequencing. Complete genotypes of all strains used in this study are provided in Table 1.

RNA electrophoresis and Northern (RNA) blot hybridization. RNA samples were prepared from 10-ml aliquots of control and 15-min heat-shocked cultures, electrophoresed, and blot hybridized to *HSC82*- and *ACT1*-specific probes as previously described (1). *HSC82* RNA was detected by using either antisense RNA probe C3 or a synthetic oligonucleotide (65-mer) homologous to its 3′ untranslated region (spanning positions +2248 to +2184) (Fig. 1B). *ACT1* RNA was detected by using a 1.6-kb antisense RNA probe homologous to its coding region. Stringent hybridization conditions (65°C hybridization and wash for C3, 45°C hybridization and wash for the 65-mer) that eliminated cross-hybridization between *HSC82* and its closely related homolog, *HSP82*, were used. *HSC82* transcript levels (Table 2) were quantitated by laser densitometry of autoradiograms and by PhosphorImager analysis; they were internally normalized to *ACT1* levels as described previously (40). Moreover, the residual background signal detectable in the *hsc82*Δ control strain, CRY102, was subtracted from each value (C3 hybridizations).

Nuclease digestion of chromatin, agarose DNA electrophoresis, and Southern blot hybridization. Cells from control and heat-shocked cultures were converted to spheroplasts as previously described (1). Washed spheroplasts were lysed and digested with DNase I, and the resultant DNA was purified, restricted with *Bam*HI, electrophoresed, transferred to GeneScreen, and subjected to indirect end labeling using riboprobe C1 as before. Similarly, the micrococcal nuclease (MNase) indirect end-labeling analysis of isolated nuclei (Fig. 9) was conducted as previously described (15). For the MNase nucleosome-protected ladder analysis (Fig. 8), nuclei were isolated from 100-ml aliquots of early-log-phase cultures (~10^7 cells per ml) and digested at 37°C for 10 min with 30, 60, 120, or 240 U of MNase (control) or 60 and 120 U of MNase (heat shocked). Mapping of cleavage sites for all indirect end-labeling experiments (Fig. 6, 7, and 9) was facilitated by the coelectrophoresis of landmark fragments, which were prepared by digesting wild-type (WT) genomic DNA with *Bam*HI alone (+4100) or in combination with *Eco*RI (−615), *Hin*dIII (−370), *Xba*I (−285, −173), or *Kpn*I (+325, +553).

***Taq*I accessibility assay.** Nuclei, isolated from a 500-ml early-log-phase culture as described above, were suspended in 2.0 ml of *Taq*I nuclear digestion buffer (50 mM NaCl, 6 mM $MgCl_2$, 10 mM Tris-HCl [pH 7.6]) and digested at 41°C for 20 min with *Taq*I, using 4 or 12 U of enzyme per μg of nuclear DNA. Note that under these conditions, which were derived to preserve native chromatin structure, *Taq*I is limiting (see Fig. 7B, lanes 1 and 2). To control for variable recovery of nuclei, we quantified the amount of DNA in each sample spectrophotometrically prior to addition of enzyme. A 5-μl aliquot of nuclear suspension was mixed with 495 μl of 1 N NaOH; the nuclear DNA concentration (in milligrams per milliliter) of the undiluted sample was estimated by using the formula ($A_{260} - 1.6 \times A_{320}$)/27. Digestions were terminated through addition of EDTA to 5 mM and genomic DNA purified as described above. The genomic DNA was then restricted with *Bam*HI, electrophoresed through a 1.8% agarose gel, and blotted to nylon, and *HSC82*-specific fragments were illuminated by hybridization with probe C1. Relative accessibility was calculated by dividing the signal of the −140 band by the combined signal of the parental +4100 band and the −140 band. Band intensities were quantitated with a PhosphorImager.

Genomic footprinting analyses. Nucleotide resolution analysis of genomic DNA purified from DNase I-digested spheroplast lysates was performed by using amplified primer extension (AMPEX) as previously described (15). To map residues protected from or hyperreactive to dimethyl sulfate (DMS) in vivo methylation, we modified the ligation-mediated PCR procedure of Giardina and Lis (23) for AMPEX. Briefly, yeast strains were grown in 250-ml cultures to early log phase, harvested by centrifugation, and then resuspended in YPD to a total volume of 2.5 ml. The sample was then divided into five aliquots, which were either maintained at 23°C (nonshocked) or placed in a 39°C water bath for 15 min (heat shocked). DMS was then added to a final concentration of 0.1, 0.2, 0.4, or 0.8% for 1 min; each suspension was rapidly agitated at either 23 or 39°C. Methylation reactions were terminated through addition of an equal volume of stop buffer (1 M sorbitol, 0.1 M Tris-HCl [pH 8.0], 0.1 M EDTA, 20 mM sodium azide, 100 mM β-mercaptoethanol). Cells were pelleted, washed a second time in 1.2 M sorbitol–0.1 M Tris-HCl [pH 8.0]–1 mM EDTA–20 mM sodium azide–40 mM β-mercaptoethanol, and then spheroplasts were prepared and DNA was isolated as previously described for the AMPEX procedure (15).

Control naked genomic DNA, purified through a Sephadex G-50 spin column and dissolved in 20 mM Tris-HCl (pH 7.5)–5 mM $MgCl_2$, was reacted with 0.2 to 1.6% DMS at 23°C for 2 min. Reactions were terminated through addition of an equal volume of stop buffer (1.5 M sodium acetate, 1 M β-mercaptoethanol), and DNA was recovered by ethanol precipitation. In this protocol, sites of DMS modification are revealed irrespective of piperidine treatment; the data presented in Fig. 5 were obtained from samples in which piperidine treatment was withheld. The *HSC82*-specific oligonucleotides used to generate the DMS in vivo footprints shown in Fig. 5 were 5′-TGCATGTGTTCATGTCACTTACGG-3′ (spanning nucleotides −46 to −69 of the lower strand) and 5′-CTTTTTGTAT TCATAGAACAGCAGCC-3′ (spanning nucleotides −273 to −248 of the upper strand). The DNase I genomic footprints depicted in Fig. 4 were generated using a +25→+2 primer as previously described (15).

Purification of GST-ScHSF and in vitro footprinting assay. A glutathione *S*-transferase (GST)-*HSF1* fusion gene was constructed by blunt-end ligation of the *Pvu*II-*Xho*I *HSF1* fragment into a *Sal*I-cut pGEX-2T vector (Pharmacia). This manipulation resulted in the in-frame fusion of the 26-kDa GST moiety with the 88-kDa ScHSF open reading frame; 14 amino acids bridge the two open

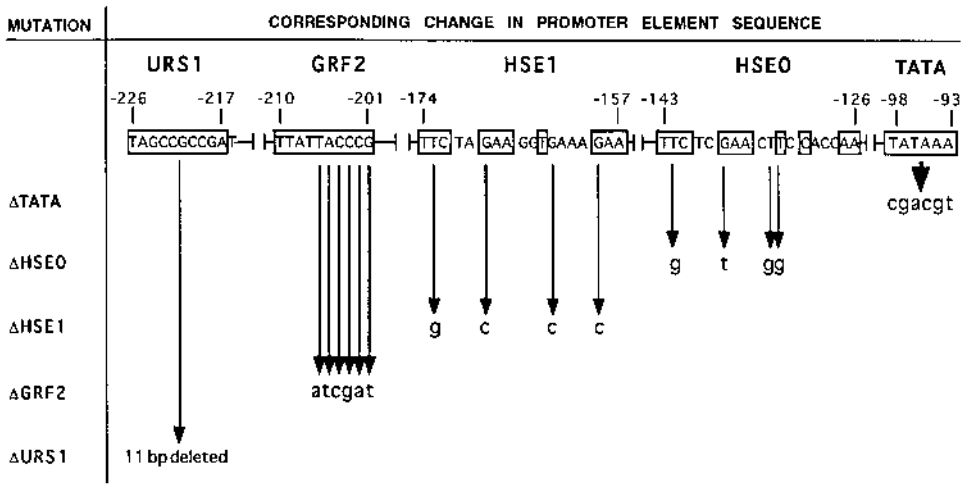

FIG. 2. Nucleotide substitutions and deletions introduced into *HSC82* promoter elements. Conserved nucleotides found within each regulatory sequence are boxed. Isogenic *hsc82* strains constructed in this study harbor one or more of these *cis*-acting mutations (Tables 1 and 2).

reading frames. GST-ScHSF (judged intact by Coomassie blue staining and immunoblotting with an anti-ScHSF polyclonal antibody) was overproduced in *Escherichia coli* BL21 and purified essentially as described previously (22a) except that isolation conditions were scaled up for a 1-liter culture (typical yield was ~100 μg). Binding reactions were conducted in 150 mM NaCl–1 mM $CaCl_2$–3 mM $MgCl_2$–20 mM Tris-HCl (pH 8.0)–0.5 mM EDTA–1 mM phenylmethylsulfonyl fluoride–100 μg of bovine serum albumin per ml as described previously (5).

RESULTS

In situ mutagenesis of the upstream region reveals critical roles for the HSE1, GRF2, and TATA elements in regulating *HSC82* transcription. To investigate the functional role of promoter elements stably occupied by protein in vivo, we constructed isogenic *hsc82* strains harboring mutations in the promoter-distal HSE (HSE1), the GRF2/REB1 motif, or the TATA box (*HSC82* promoter sequence and a summary of genomic footprinting data are presented in Fig. 1A; a physical map of the gene and locations of hybridization probes are provided in Fig. 1B). Moreover, two additional mutant strains were constructed: one in which the promoter-proximal HSE, HSE0, was disrupted, and another in which the consensus upstream repressor sequence, URS1, was deleted (Fig. 2). These latter two elements are not detectably protected from DNase I and are at best weakly protected from DMS (see below). As summarized in Table 2, a 4-bp substitution within HSE1 reduces *hsc82* transcript levels 25-fold in nonshocked cells and >100-fold in heat-shocked cells (strain HSE101). Similarly, a 6-bp substitution of the TATA motif reduces *HSC82* transcription ~5-fold irrespective of heat shock (strain TAT100), while a comparable mutation in the GRF2 site causes a 70% diminishment of basal transcription and a nearly 50% drop in induced transcription (strain GRF200). In contrast, a 4-bp mutation within HSE0 exhibits only a mild heat shock phenotype (having no impact on basal expression), despite this sequence exhibiting as strong a match to the HSF consensus sequence as HSE1 (strain HSE100; see the legend to Fig. 1). Strains harboring multiple promoter mutations were also made. Their phenotypes were as expected: HSE102, a strain harboring mutations in each HSE, and TAT101, a strain containing mutations in both HSE1 and TATA, each exhibit a

TABLE 2. *HSC82* mutant strains and summary of structural and functional phenotypes[a]

Strain	Promoter mutation(s)	Normalized RNA level[b]		Effect on promoter accessibility[c]	Effect on nucleosome positioning[d]
		NHS	HS		
W303-1B	None (*HSC82*$^+$)	100	250	−	−
TAT100	Substituted TATA (ΔTATA)	20	45	*	−
TAT101	ΔTATA + ΔHSE1	2	<1	++	−
TAT102	ΔTATA + ΔHSE1 + ΔURS1	1	<1	++	ND
HSE100	Substituted HSE0 (ΔHSE0)	90	140	−	−
HSE101	Substituted HSE1 (ΔHSE1)	4	2	++	−
HSE102	ΔHSE0 + ΔHSE1	2	<1	++	−
GRF200	Substituted GRF2 (ΔGRF2)	30	140	+	+
URS100	Deleted URS1 (ΔURS1)	90	210	−	+
URS101	ΔURS1 + ΔHSE0	100	170	−	ND
URS102	ΔURS1 + ΔHSE1	2	2	++	+
URS103	ΔURS1 + ΔHSE0 + ΔHSE1	1	1	++	ND

[a] Values represent the means of at least two or three independent preparations.
[b] NHS, non-heat shocked; HS, heat shocked.
[c] −, WT frequency of DNase I or *Taq*I cleavage; *, enhanced frequency of *Taq*I cleavage; +, mild reduction in nuclease cleavage; ++, severe reduction in nuclease cleavage.
[d] −, WT location of 5′ flanking nucleosomes; +, 10- to 20-bp translational shift in the position of the upstream nucleosomal array; ND, not determined.

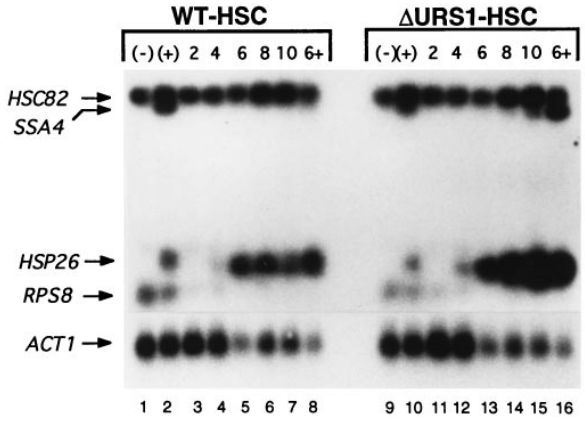

FIG. 3. Deletion of URS1 does not block meiotic induction of *HSC82*. RNAs were extracted from aliquots of cultures of the diploid strains WT-HSC and ΔURS1-HSC at various times after transfer to nitrogen-deficient sporulation medium. Fifteen micrograms of purified RNA from each sample was separated on a 1.1% agarose-formaldehyde gel and transferred to nylon. *HSC82*, *SSA4*, *HSP26*, *RPS8*, and *ACT1* transcripts were detected as previously described (1); in particular, *HSC82* transcripts were detected by using probe C3. Lanes: (−), control cells grown in synthetic acetate (presporulation) medium at 30°C; (+), cells grown in presporulation medium and subjected to a 15-min heat shock at 39°C; 2 to 10, hours after transfer to nitrogen-deficient sporulation medium; 6+, 6-h sample subjected to a 39°C heat shock for 15 min. Densitometric quantitation reveals that in both strains, *HSC82* transcript levels (internally normalized to the *ACT1* level) increase two- to threefold at 6 h, plateauing thereafter. Heat shock superimposed upon nitrogen starvation results in a further 10 to 30% increase in *HSC82* RNA levels (lanes 8 and 16).

more severe phenotype than their singly mutated counterparts (Table 2). We conclude that while the HSE1, GRF2, and TATA sequences play critical regulatory roles under these growth conditions, HSE0 does not.

The URS1 element can be deleted without altering *HSC82* expression during either mitotic or meiotic growth. Sequences bearing homology to the URS1 upstream repressor sequence are found 5′ of a number of regulated yeast genes, including the *SSA1* and *HSP82* heat shock genes (52, 64). Genetic analyses have indicated that the URS1 motif, which is normally located between the upstream activation sequence (UAS) and the TATA element, functions as a repressor in mitotic cells (63). To test the function of the URS1 element at *HSC82*, we constructed isogenic strains bearing a deletion of this sequence alone and in combination with mutations in other promoter elements. URS1 is positioned 50 bp upstream of HSE1 (Fig. 1A) and is only weakly protected from DMS in vivo methylation (see below) despite exhibiting a 10/10 match to the consensus (47, 64). In logarithmically growing cells, there is no detectable phenotype associated with the URS1 deletion in any one of the four strains in which it was introduced (URS100 to URS103). This is most clearly seen in the absence of other *cis*-acting mutations (strain URS100), where *HSC82* RNA levels are essentially indistinguishable from those in the WT strain, W303-1B (Table 2).

As the URS1 element has been shown to positively regulate meiosis-specific genes (9, 49, 64), we asked whether *HSC82* was induced during sporulation and, if so, whether the URS1 deletion had any effect on this induction. To test this, we constructed two diploid strains that were heterozygous with respect to the *hsc82* allele, WT-HSC (*HSC82*$^+$/*hsc82*Δ*::URA3*) and ΔURS1-HSC (*hsc82-*Δ*URS1*/*hsc82*Δ*::URA3*). Northern analysis of WT-HSC cells reveals that the high constitutive level of *HSC82* is induced severalfold following a shift to nitrogen-free medium, peaking between 6 and 10 h. This level of induction is comparable to what is seen during a brief heat shock (Fig. 3; compare lanes 5 to 7 with lane 2). Indeed, no further induction is seen when sporulating cells are subjected to a 15-min heat shock (lane 8). That this induction reflects an early meiotic rather than general starvation response is suggested by the fact that *HSC82* is not induced in the WT haploid strain subjected to the identical regimen (data not shown). Surprisingly, an essentially identical expression pattern is seen in strain ΔURS1-HSC (lanes 9 to 16), ruling out a role for URS1 in regulating the meiotic induction of *HSC82* transcription. Confirmation that these diploid strains were indeed sporulating was obtained by both cytological and molecular analyses. The fraction of cells in which two, three, or four spores were visible increased from 0% at 2 h to >50% at 10 h (>90% at 24 h). Similarly, rehybridizing the RNA samples with probes specific for other meiotically induced genes revealed that within 4 to 6 h after the shift to sporulation medium, both *HSP26* and *HSP82* were strongly induced (Fig. 3 and data not shown), as previously seen (36, 64). In contrast, *SSA4* was not measurably activated (although it was induced by heat shock), while the ribosomal protein gene *RPS8* was strongly repressed early during sporulation (Fig. 3, lanes 3 and 11), as observed by others (70). Taken together, these data suggest that *HSC82* is a meiotically induced gene whose activation can occur in the absence of URS1.

Genomic footprinting indicates a role for the GRF2-binding factor in facilitating occupancy of HSE1 and TATA elements. To investigate the effect of mutating upstream regulatory elements on protein-DNA interactions, we mapped sites of DNase I cleavage and DMS modification within *hsc82* promoter mutants at nucleotide resolution. Spheroplast lysates, generated from WT and three promoter mutant strains (GRF200, HSE101, and URS101), were digested with DNase I, and genomic DNA was purified and subjected to AMPEX. As illustrated in Fig. 4A, within the WT upstream promoter region, HSE1 is strongly protected from DNase I (irrespective of heat shock) and GRF2 is moderately protected, while URS1 and HSE0 are not detectably protected (compare lanes 3 and 4 with lane 2). As expected, DNase I protection is abolished at the mutated sites within the ΔGRF2 and ΔHSE1 strains. Interestingly, this assay also suggests that there is a diminished interaction at HSE1 in the ΔGRF2 mutant. This interpretation is based on the loss of protection at position −167, a site that is strongly cleaved in naked DNA and almost completely protected in WT chromatin (filled circle), as well as a reduction in flanking hyperreactivity. Notably, there is no comparable effect on the HSE1 footprint in the ΔURS1 ΔHSE0 double-mutant strain (lane 16), arguing that HSF binding to HSE1 is independent of both URS1 and HSE0 sites. Likewise, strong DNase I protection is retained at the GRF2 site in the ΔHSE1 strain (lanes 11 and 12), suggesting that the GRF2 factor can bind to the *hsc82* promoter independently of HSF.

To confirm the GRF2 effect on HSE1 occupancy in intact cells, we used DMS in vivo footprinting. Cells were concentrated in rich medium and briefly reacted with DMS at either 23°C (control) or 39°C (heat shocked). Following purification of genomic DNA, sites of purine methylation were mapped by using AMPEX. Two sites of constitutive protection are evident within the *HSC82*$^+$ upstream promoter: HSE1 and GRF2 (Fig. 5A, lanes 4 and 5, and Fig. 5B, lanes 4 and 5; protections denoted by striped bars). These two regions of protection are flanked by hyperreactive purine residues on the lower strand (arrowheads; data summarized in Fig. 1A). In the isogenic ΔGRF2 strain, in addition to the expected loss of protections and enhancements associated with the mutated site, reduced DMS protection is seen at each of the three consensus GAA modules within HSE1, at positions −159 and −169 on the upper strand and at position −172 on the lower strand; more-

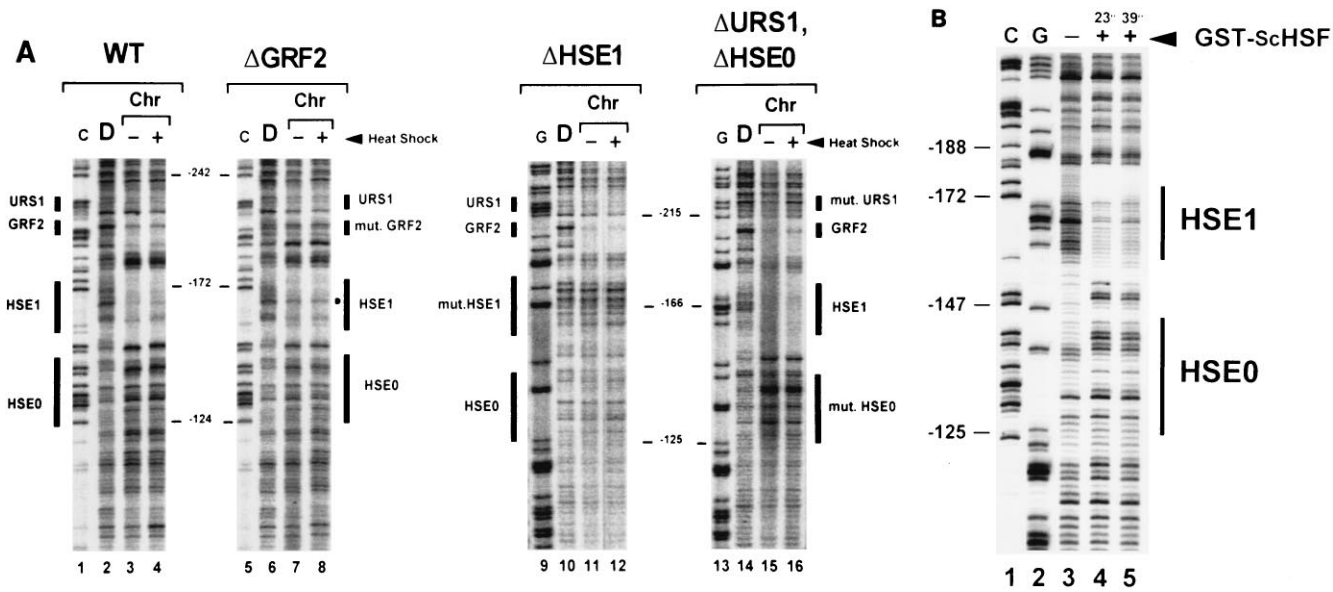

FIG. 4. DNase I genomic footprinting analysis of WT and mutant *hsc82* alleles. (A) Spheroplast lysates of W303-1B (*HSC82*$^+$), GRF200 (*hsc82*-ΔGRF2), HSE101 (*hsc82*-ΔHSE1), and URS101 (*hsc82*-ΔURS1, ΔHSE0) were generated from control (−) and 15-min heat-shocked (+) cultures and digested with DNase I, and genomic DNA was purified and subjected to reiterative primer extension for 10 cycles, using an oligonucleotide complementary to the *HSC82* upper strand (spanning +25 to +2). Products were resolved on 8% sequencing gels as previously described (15). Chr, chromatin (spheroplast lysates); mut., mutated; D, naked genomic DNA digested with DNase I; C and G, dideoxy sequencing ladders. Designations refer to upper-strand sequence. Note that lanes 1 to 8 were derived from one gel, while lanes 9 to 16 were from another. Nucleotide positions relative to the principal transcription start site are indicated. (B) In vitro footprinting analysis of recombinant ScHSF bound to the WT promoter. Approximately 50 nM recombinant polypeptide was allowed to react with 3.5 nM DNA template in standard binding buffer for 45 min at either 23 or 39°C as indicated. The resultant protein-DNA complex was digested with DNase I for 1 min, the reaction was terminated, and DNA was purified by organic extraction. The purified DNA was subjected to 10 cycles of primer extension using the +25→+2 primer. The DNA template was CAM105, a supercoiled plasmid containing a 1.65-kb insert spanning the *HSC82* upstream region. Lanes 1 and 2, sequencing ladders; lanes 3 to 5, DNase I-digested template, either in the absence (−) or in the presence (+) of GST-ScHSF.

over, the hyperreactivity mapping to the nearby −183 G residue is lost (lanes 9 and 10 in both panels). A quantitative analysis of the HSE1 region is shown in Fig. 5C, confirming that both major and minor groove protections (G and A residues, respectively) are reduced in the GRF2 mutant. Interestingly, loss of protection appears to be equally pronounced in control and heat-shocked cells. Taken together, the genomic footprinting data argue that the GRF2-binding protein assists and/or stabilizes the interaction of HSF within the *HSC82* upstream region.

Dependence of HSF on the GRF2 element for stable binding raises the question of whether downstream factors, TATA-binding protein (TBP) in particular, are similarly dependent. As illustrated in Fig. 5D, the ΔGRF2 mutation also materially reduces the level of protection of adenines within the TATA box to DMS relative to that seen in the WT promoter. DMS methylates adenines on the N-3 moiety within the minor groove, the site of TBP binding (31). As above, this diminished level of protection is equally pronounced in nonshocked and heat-shocked cells and implies a further role for the GRF2-binding protein in the stabilization of the TBP-TATA interaction (see Discussion).

A 4-bp mutation in HSE1 abolishes in vivo occupancy of the TATA box. Given the profound expression phenotype associated with the ΔHSE1 lesion, we tested whether the HSE1 mutation would also affect the TBP-TATA interaction. We anticipated that this might be the case, in light of the above result with the ΔGRF2 strain as well as previous results implicating a central role for HSF in facilitating occupancy of the TATA box at *HSP82* (24). Indeed, as illustrated by the scans in Fig. 5D, all minor groove interactions mapping to the TATA motif are abolished upon mutation of HSE1. Evidence presented below suggests that the TBP-TATA interaction is replaced by a stable nucleosome localized over the core promoter region. Notably, the reciprocal effect is not seen: a 6-bp substitution of the TATA element, despite significantly lowering transcript levels (Table 2), has no detectable effect on the occupancy of either HSE1 or GRF2 (Fig. 5C and data not shown). This finding argues that factors binding to these upstream sequences can do so independently of stably bound TBP.

The ScHSF in vitro footprint strongly resembles its genomic counterpart. Given the central importance of the HSE1 protein complex in regulating both the expression and the structure of *HSC82* (Table 2 and Fig. 6 to 8), we wished to determine whether HSF was solely responsible for the protection seen or whether factors in addition to HSF contribute to the footprint. To test this directly, we reacted a GST-ScHSF fusion protein with a supercoiled template bearing the *HSC82* upstream region. As illustrated in Fig. 4B, the footprint of the recombinant protein is essentially identical to the HSE1 genomic footprint, with respect to both the breadth of protection (spanning −180 to −150) and the presence of flanking hyperreactivity (Fig. 4A and reference 15). Notably, at an HSF concentration sufficient to strongly protect HSE1, no protection is seen within HSE0 (Fig. 4B). Interestingly, GST-ScHSF binds HSE1 under both control and inducing temperatures, resembling the in vivo activity of the native factor but contrasting with the behavior of a mouse GST-HSF fusion protein which binds DNA only following a heat-induced conversion (23a). We conclude that the protection conferred by HSF can fully account for the HSE1 genomic footprint and that the absence of protection at HSE0 reflects the intrinsically low affinity of HSF for this site.

Mutation of HSE1 abolishes promoter-associated DNase I hypersensitivity and restricts accessibility to *Taq*I endonuclease. To investigate the effects of the promoter mutations on

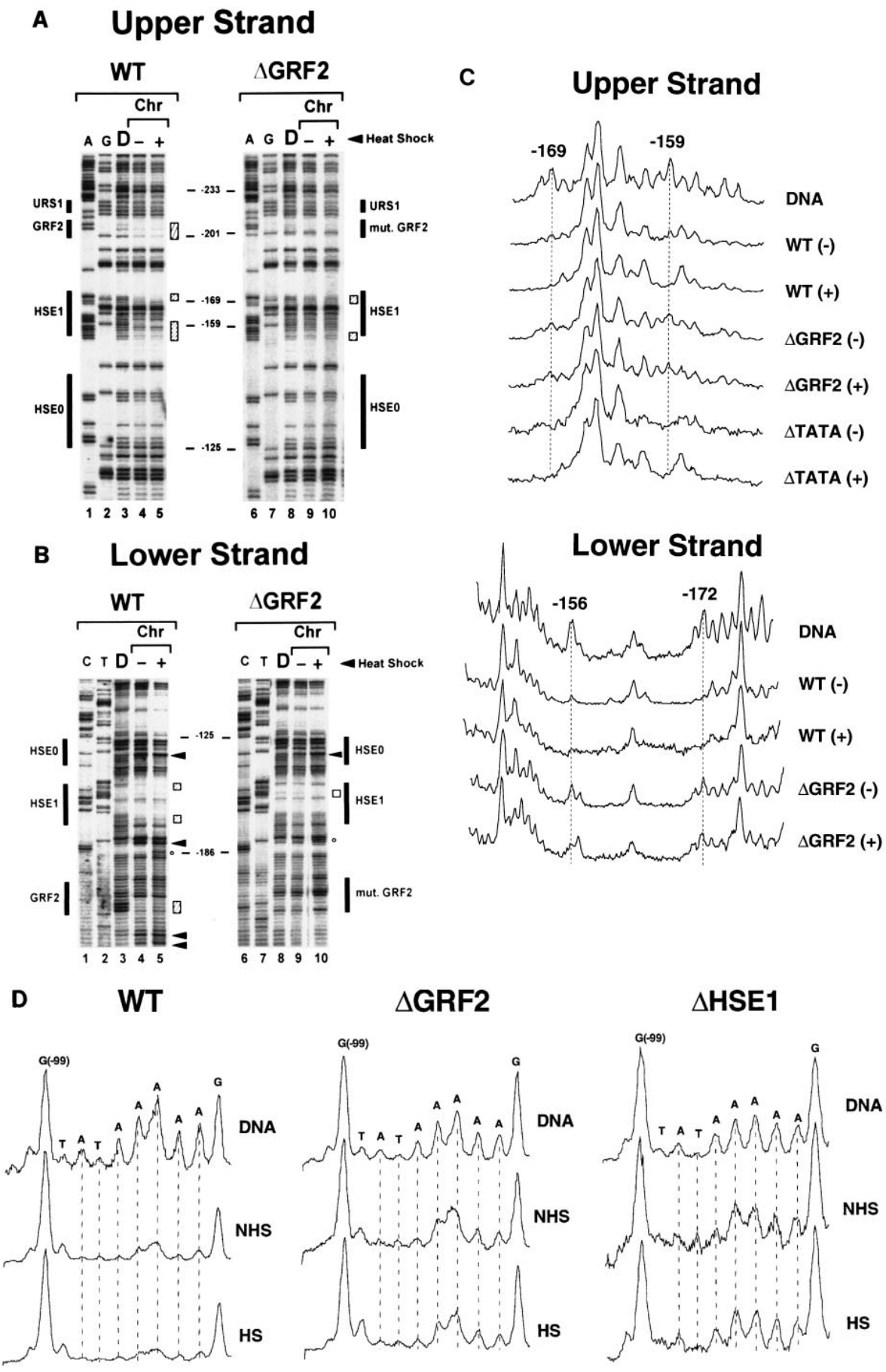
A
Upper Strand
WT
ΔGRF2
Chr
A G D – +
Heat Shock
URS1
GRF2
HSE1
HSE0
mut. GRF2
-233
-201
-169
-159
-125
1 2 3 4 5
6 7 8 9 10
B
Lower Strand
C T D – +
-186
C
-169
-159
DNA
WT (-)
WT (+)
ΔGRF2 (-)
ΔGRF2 (+)
ΔTATA (-)
ΔTATA (+)
-156
-172
D
ΔHSE1
G(-99)
T A T A A A A G
NHS
HS

FIG. 5. Mutation of the GRF2 site attenuates protein-DNA interactions at both HSE1 and the TATA box as revealed by DMS in vivo footprinting. (A) Intact cells, concentrated from nonshocked (−) or 15-min heat-shocked (+) cultures of WT and ΔGRF2 strains, were briefly reacted with DMS at 23 or 39°C, respectively. Genomic DNA was then purified and subjected to AMPEX using an upper-strand-specific oligonucleotide spanning −46 to −69, and the product was resolved on an 8% sequencing gel. (B) Same as panel A except that AMPEX was performed with a lower-strand-complementary oligonucleotide spanning −273 to −248. Chr, chromatin (intact cells); other abbreviations are as for Fig. 4. Symbols are as for Fig. 1A except here an open bar designates heat shock-inducible DMS protection. (C) Densitometric analysis of the HSE1 region. Dashed lines indicate G residues strongly protected from DMS in WT and ΔTATA but not ΔGRF2 cells. Positions −172, −169, and −159 correspond to the consensus GAA modules within HSE1. (D) Densitometric analysis of the TATA region. Scans were internally normalized with respect to the −99 G signal, which was set to the same amplitude in all samples. DNA, purified genomic DNA; NHS, non-heat shocked; HS, heat shocked.

local chromatin structure, we mapped regions of DNase I accessibility by indirect end labeling. As shown in Fig. 6, the broad DNase I-hypersensitive region spanning the WT promoter (lanes 1 and 2) is drastically reduced in intensity at the *hsc82*-ΔHSE1 allele (lanes 3 and 4). That the hyperreactive cleavages are chromatin specific has been confirmed by a pairwise comparison with a comparably digested deproteinized genomic DNA sample (data not shown; see also reference 15). This result suggests that a dramatic reduction in promoter accessibility accompanies the 4-bp mutation within HSE1. In contrast, a comparable 4-bp substitution mutation within HSE0 has virtually no effect on the DNase I cleavage profile of the gene (lanes 7 and 8). This result is consistent with measurements of steady-state *HSC82* RNA levels (Table 2) which indicate that the HSE0 mutation has at best a mild phenotype, as well as genomic footprinting analyses of the wild-type allele which argue against the presence of stably bound protein at this site (Fig. 4 and 5) (15). Also consistent with the absence of an expression phenotype, robust nuclease hypersensitivity is retained in the URS1 deletion strain (lanes 5 and 6). Importantly, the chromatin samples derived from ΔHSE0, ΔURS1, and ΔHSE1 strains are digested to comparable degrees, yet promoter-associated DNase I hypersensitivity is clearly retained in the former two strains but nearly abolished in the latter (compare lanes 5 to 8 with lanes 3 and 4). Moreover, despite strongly affecting *hsc82* transcription, mutations in either TATA or GRF2 do not detectably alter the promoter-associated DNase I-hypersensitive site (data not shown). We conclude that in contrast to the HSE1 substitution, mutations of the other four elements have relatively little impact on promoter chromatin structure, even when they are present in combination (data not shown; see Table 2 for a summary of phenotypes).

To strengthen the foregoing conclusions, we examined whether the TCGA sequence at position −140, unique to the *HSC82* upstream region and located within the promoter-associated DNase I-hypersensitive site, would be accessible to *Taq*I in isolated nuclei. Restriction enzyme cleavage is severely limited in nucleosomal DNA (3); thus, we reasoned that if the nucleosome-free (or nucleosome-disrupted) state of the WT promoter were preserved at the mutant *hsc82* alleles, the promoter chromatin would remain accessible to *Taq*I. However, if this open chromatin configuration were replaced by a nucleosomal structure, *Taq*I accessibility would be reduced or lost. As anticipated, the −140 site is highly accessible in WT chromatin (Fig. 7A, lanes 2 to 5; Fig. 7B, lanes 3 to 6). In contrast to the DNase I hypersensitivity assay, however, the extent of *Taq*I cleavage appears to increase nearly twofold following heat shock (most clearly seen in Fig. 7A, lanes 4 versus 2 and 5 versus 3). Interestingly, the nine TCGA sites spanning the *HSC82* transcription unit are relatively inaccessible to *Taq*I, particularly in nonshocked nuclei (compare WT samples with naked DNA [Fig. 7B, lanes 3 and 4 versus lanes 1 and 2]). This observation is consistent with previous observations indicating the presence of a canonical nucleosomal array over the coding region of this gene (15).

Strong *Taq*I cleavage is also apparent within the *hsc82*-ΔGRF2 promoter region (Fig. 7A, lanes 10 to 13). Note that this allele has two promoter-associated TCGA sites, the naturally occurring one at position −140 and a synthetic site at −205 (Fig. 1B and 2). The combined cleavage frequency of the two *Taq*I sites is slightly less than the frequency of cleavage of the single *Taq*I site in WT nuclei; following heat shock, they are essentially equivalent. Given that under these conditions *Taq*I is limiting (Fig. 7B, lanes 1 and 2; see Materials and Methods), such a comparison permits the conclusion that the ΔGRF2 mutation has only a modest effect on the accessibility of the promoter region to *Taq*I. Similarly, despite reducing *HSC82* transcript levels ~80% (Table 2), substitution of the TATA box does not curtail accessibility of the promoter region to *Taq*I. Instead, cleavage of the −140 site is enhanced twofold in strain TAT100 compared to WT under both nonshock and heat-shocked conditions (Fig. 7B; compare lanes 7 to 10 with lanes 3 to 6). In marked contrast, the −140 *Taq*I site in strain HSE101 is only 15% (heat shock) to 35% (nonshock) as frequently cleaved as it is in WT nuclei (Fig. 7A; compare lanes 8 and 9 with lanes 4 and 5 and lanes 6 and 7 with lanes 2 and 3), indicating that a drastic reduction in promoter accessibility accompanies mutagenesis of HSE1, particularly following heat shock. This result is fully consistent with the reduction of

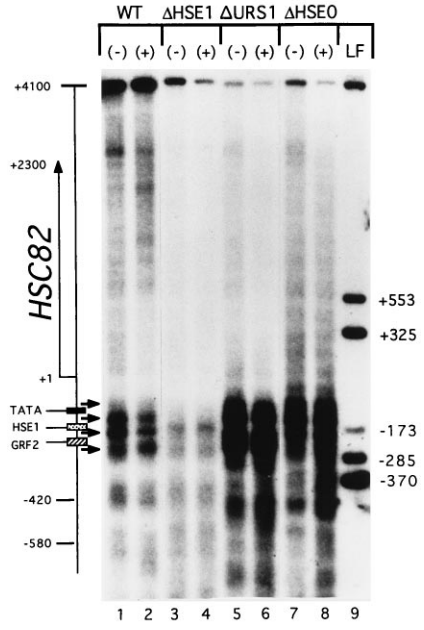

FIG. 6. A 4-bp mutation within HSE1 abolishes the promoter-associated DNase I-hypersensitive region, while comparable mutations within either HSE0 or URS1 do not. DNase I cleavage profiles from WT (lanes 1 and 2) and promoter mutant strains (lanes 3 to 8) were visualized by indirect end labeling with probe C1. Arrows indicate regions of intense DNase I cleavage. Locations of regulatory elements are shown at left; regions of protection (footprints) in the wild-type promoter are indicated by rectangles. LF, landmark fragments.

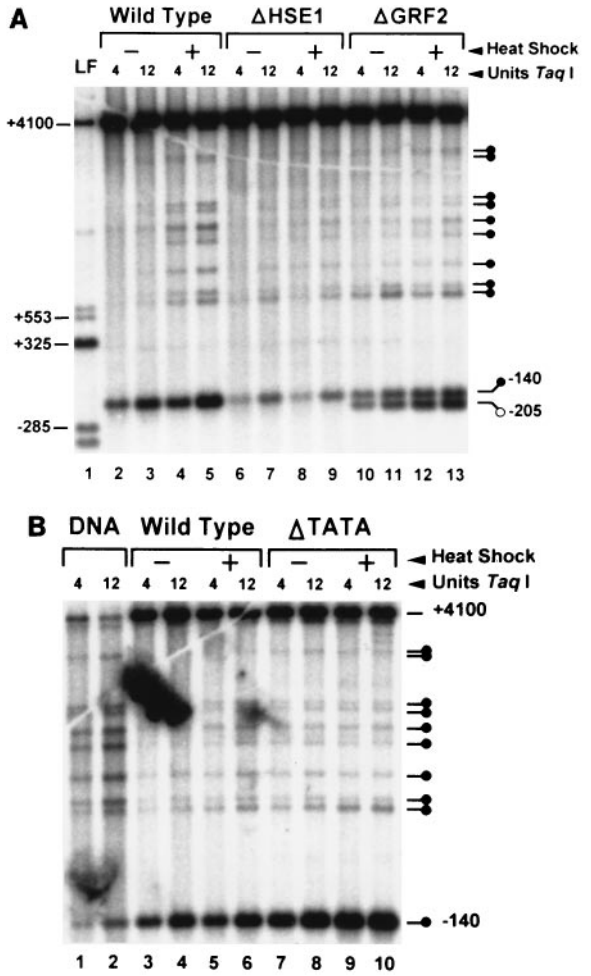

FIG. 7. The ΔHSE1 mutation severely reduces accessibility of the *hsc82* promoter to *Taq*I, while a comparable mutation in TATA increases it. (A) Nuclei were isolated from control and heat-shocked W303-1B (lanes 2 to 5), HSE101 (lanes 6 to 9), and GRF200 (lanes 10 to 13) cells and digested at 41°C with the indicated amount of *Taq*I per microgram of nuclear DNA for 20 min. DNA was purified, restricted with *Bam*HI, electrophoresed, and blot hybridized with probe C1. Locations of naturally occurring *Taq*I sites (at positions −140, +679, +766, +1015, +1381, +1474, +1576, +1612, +1867, and +1969) are indicated with filled circles; the synthetic site at position −205, unique to the *hsc82*-ΔGRF2 allele, is indicated by an open circle. LF, landmark fragments. (B) Nuclei purified from W303-1B (lanes 3 to 6) and TAT100 (lanes 7 to 10) cells were digested with *Taq*I, and DNA was prepared as described above. Naked genomic WT DNA (lanes 1 and 2) was digested under identical conditions. Symbols are as for panel A.

DNase I hypersensitivity demonstrated above. Taken together, the DNase I hypersensitivity and *Taq*I accessibility assays argue that the HSE1 mutation severely restricts promoter accessibility, whereas comparable mutations in GRF2, TATA, HSE0, and URS1 do not.

A 4-bp mutation in HSE1 leads to a well-resolved nucleosome-protected ladder, while mutations in other promoter elements do not. The dramatic loss of DNase I hypersensitivity and *Taq*I accessibility accompanying the HSE1 mutation suggests that this lesion affects the nucleosome-free state of the *hsc82* promoter region. To more directly address this possibility, we digested nuclei isolated from *HSC82* and *hsc82*-ΔHSE1 cells with MNase, a sensitive probe of nucleosomal structure. Genomic DNA was purified, electrophoretically resolved, and blotted to nylon, and *hsc82* promoter-specific fragments were visualized by hybridization to probe C2. As previously demonstrated (15), MNase excises a novel fragment of ~210 bp from the WT promoter region with or without heat shock (Fig. 8, lanes 1 to 6). In contrast, when a similar treatment is performed on nuclei isolated from strain HSE101, a stable, nucleosome-length fragment of ~170 bp is detected, as part of a larger, well-resolved ladder exhibiting a repeat length of 170 ± 5 bp (lanes 8 to 13). Notably, this difference between WT and mutant profiles is maintained irrespective of the level of digestion, arguing that the difference in monomer lengths is not an artifact of MNase exonuclease activity. To further validate the difference between the two strains, in an independent experiment we eluted probe C2 from the membrane and reprobed the DNA samples with C1, which is homologous to a region of intergenic chromatin centered approximately 1 kb upstream of *HSC82* (Fig. 1B). We found that for each strain, the monomer-length fragment derived from intergenic chromatin exhibited precisely the same mobility as the monomer fragment excised from the mutated, but not WT, promoter (data not shown). This result is therefore consistent with the DNase I and *Taq*I experiments: all three indicate that a 4-bp mutation in HSE1 is associated with a striking structural phenotype. Similar analyses of *hsc82* strains bearing promoter mutations in URS1, GRF2, HSE0, or TATA resulted in MNase ladders whose patterns were indistinguishable from the WT pattern (data not shown). We conclude that HSE1, unique among the regulatory elements tested, is critically required for maintaining the promoter region in a nucleosome-free (or nucleosome-disrupted) state.

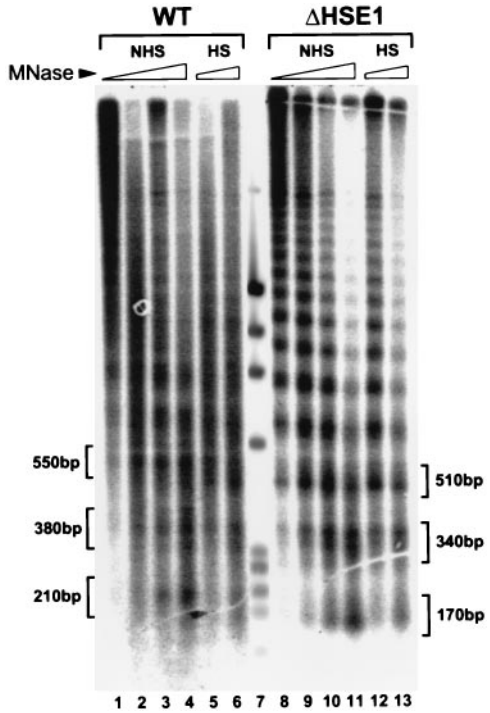

FIG. 8. Mutagenesis of HSE1 sharpens the nucleosome-protected ladder over the *hsc82* promoter region. Nuclei, isolated from nonshocked (NHS) or 15-min heat-shocked (HS) cultures of strains W303-1B and HSE101 (lanes 1 to 6 and 8 to 13, respectively), were digested with increasing amounts of MNase as indicated. The DNA was isolated, separated on a 1.8% agarose gel, blotted to a nylon membrane, and hybridized with probe C2. Brackets correspond to mono-, di-, and trinucleosome-length fragments. Sizing of DNA fragments was done by using a coelectrophoresed molecular weight standard (*Hae*III-digested ϕX174 DNA) with fragment lengths of 1353, 1078, 872, 603, 310, 281/271 (doublet), 234, 194, and 118 bp (lane 7).

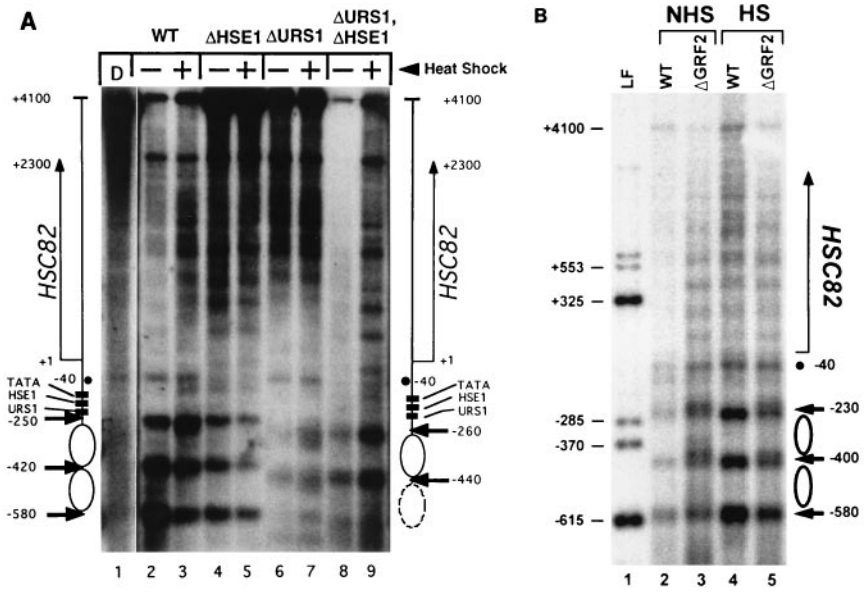

FIG. 9. Mutations within URS1 or GRF2, but not HSE1, alter the location of MNase cleavages upstream of the *hsc82* promoter. (A) MNase-cut sites in nuclei isolated from control (−) and heat-shocked (+) strains W303-1B (lanes 2 and 3), HSE101 (lanes 4 and 5), URS100 (lanes 6 and 7), and URS102 (lanes 8 and 9) were mapped by indirect end labeling using probe C1 following DNA purification and restriction with *Bam*HI. MNase-digested WT genomic DNA (D) is shown in lane 1. Boldface arrows represent regions exhibiting enhanced MNase cleavage; these sites likely correspond to the DNA linking adjacent sequence-positioned nucleosomes (symbolized by ovals). The dashed oval indicates the location of a less well positioned nucleosome. Filled circle, cleavage site specifically protected in the ΔHSE1 strain. The locations of regulatory elements within the promoter (solid rectangles) are indicated. Positions of chromatin-specific cleavages are indicated on the left for WT and on the right for ΔURS1 (independently mapped by using landmark fragments electrophoresed on outside lanes [not shown]). (B) MNase cleavage sites in nuclei isolated from W303-1B (lanes 2 and 4) and GRF200 (lanes 3 and 5) cells, non-heat shocked (NHS) and heat shocked (HS) as indicated. The locations of chromatin-specific cleavages for the ΔGRF2 strain are indicated on the right; these have been confirmed in two independent experiments. LF, landmark fragments.

Deletion of either URS1 or GRF2 shifts the location of nucleosomes positioned upstream of the hypersensitive site. Previous analysis of *HSC82* chromatin structure has suggested the presence of an upstream nucleosomal array flanking the hypersensitive site (15). To investigate the potential role of regulatory sites within the *HSC82* promoter in positioning this array, we mapped nucleosome positions in isogenic *hsc82* strains by using MNase and indirect end-labeling techniques. Three prominent, chromatin-specific cleavage sites extending upstream from the promoter and spaced at ~170-bp intervals are seen in the WT samples irrespective of heat shock (Fig. 9A, lanes 2 and 3; Fig. 9B, lanes 2 and 4), consistent with the presence of two translationally positioned nucleosomes abutting the *HSC82* regulatory region. Careful mapping of cleavage sites reveals that each is shifted at least 10 to 20 bp upstream in the ΔURS1 strain, and they are substantially more diffuse (Fig. 9A, lanes 6 and 7). Likewise, mutation of the GRF2 site shifts and diffuses the MNase cleavage profile of the upstream region, although here the two cleavages closest to the promoter (mapping to positions −230 and −400) have been shifted ~20 bp downstream (Fig. 9B; compare lanes 3 and 5 with lanes 2 and 4), suggesting a downstream shift in the promoter-proximal nucleosome. Together, these data suggest that proteins bound to the URS1 and GRF2 sites exert opposing effects on the upstream nucleosomal array.

Interestingly, disruption of HSE1 has no effect on the location or sharpness of the upstream MNase-cut sites (Fig. 9A, lanes 4 and 5), arguing that the structural role played by HSE1 does not extend upstream of the DNase I-hypersensitive region (spanning roughly positions −250 to −40). The HSE1 mutation does, however, reduce the frequency of cleavage at −40 (filled circle), a site that is detectably cut in the naked DNA sample, as well as in the WT, ΔURS1, and ΔGRF2 chromatin samples. This result is consistent with the foregoing data suggesting that the HSE1 mutation occludes promoter chromatin structure. Finally, an *hsc82* allele containing both ΔHSE1 and ΔURS1 mutations shows a pronounced upstream shift in MNase cleavage sites, virtually identical to those seen in the ΔURS1 strain (Fig. 9A, lanes 8 and 9). We conclude that the HSE1, GRF2, and URS1 elements contribute independently to the chromatin structure of the *HSC82* upstream region. While HSE1 influences primarily the core promoter region, URS1 and GRF2 exert their influence predominantly over the distal promoter and intergenic regions.

DISCUSSION

HSF creates a nucleosome-free region over the *HSC82* core promoter independently of other sequence-specific factors. We have performed a genetic dissection of transcriptional control elements found within the *HSC82* promoter region. All of our experiments were conducted in vivo on integrated transgenes, which allowed us to compare the structures and levels of expression of different *hsc82* alleles under native conditions. Our principal finding is that HSF, independently of other sequence-specific factors, creates an open chromatin configuration within the *HSC82* promoter region. This conclusion is based on three lines of evidence. First, a 4-bp substitution of HSE1, which abolishes HSF binding (Fig. 4A), abrogates promoter-associated DNase I hypersensitivity (Fig. 6) and severely reduces *Taq*I accessibility (Fig. 7A). Second, the HSE1 mutation transforms the MNase cleavage profile into a ladder of discrete mono- and oligonucleosome-length fragments. In contrast, the WT ladder is more heterodisperse and contains a nonnucleosomal, ~210-bp monomer-length fragment (Fig. 8 and reference 15). Third, mapping of MNase cleavage sites (Fig. 9A) indicates that the −40 site, sharply cleaved in WT chromatin, is protected in nuclei purified from the ΔHSE1 strain. Taken

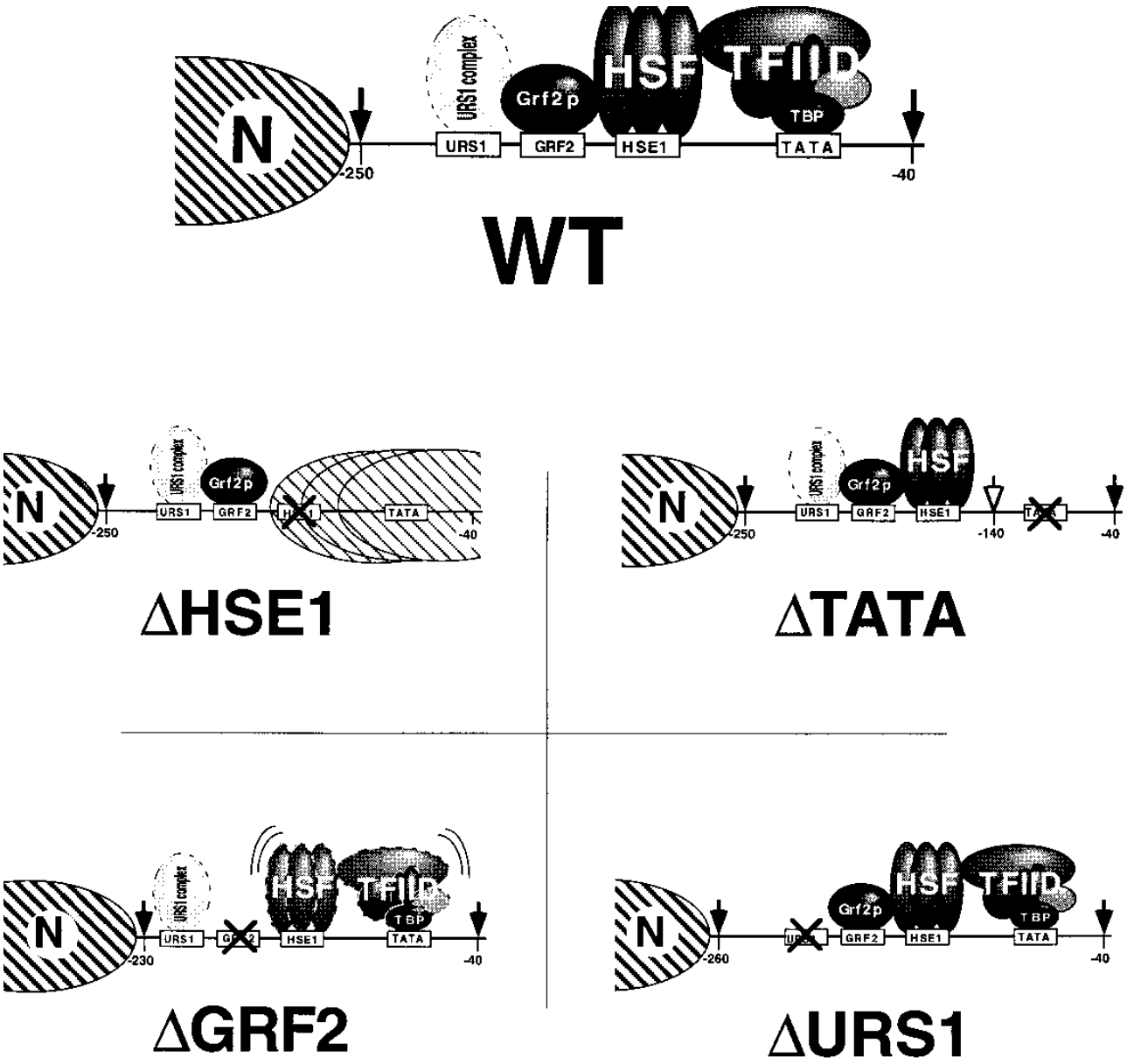

FIG. 10. Models of nucleoprotein architecture at *HSC82*$^+$ and four promoter mutants, ΔHSE1, ΔTATA, ΔGRF2, and ΔURS1. At the WT allele, strong DNase I and DMS genomic footprints mapping to GRF2, HSE1, and the TATA box suggest occupancy by Grf2p/Reb1, HSF, and TBP (depicted here as a component of the TFIID complex), respectively, while moderate DMS protection at URS1 suggests weak interaction (possibly substoichiometric) with the URS1 complex. Importantly, the promoter is in an open chromatin configuration, highly accessible to DNase I and *Taq*I. In ΔHSE1, normal sequence-specific interactions over URS1 and GRF2 are retained and perhaps even strengthened; however, the downstream region undergoes a dramatic structural transition as the HSE1-HSF and TBP-TATA interactions are lost, and the open, nuclease-hypersensitive chromatin structure is replaced by an inaccessible, nucleosome-like structure (depicted here as a single nonpositioned nucleosome). In ΔTATA, factor binding to upstream sites is at normal levels whereas accessibility of the core promoter to *Taq*I is enhanced twofold (open arrow). In ΔGRF2, factors bound to both HSE1 and TATA are destabilized (symbolized by parallel curved lines), while the upstream nucleosome is shifted ~20 bp toward the promoter. In ΔURS1, the nucleoprotein architecture over the core and upstream promoter regions is preserved whereas the translational setting of the upstream nucleosome is shifted at least 10 bp upstream. Closed arrows indicate the location of strong MNase cleavages within chromatin. HSF is depicted as a homotrimer (61), and Grf2p is depicted as a monomer (50). URS1-binding proteins are depicted as an ill-defined complex, which may consist of Ume6p or BUF (49). Note that in all five alleles, the structures shown remain essentially unchanged following heat shock. Nucleoprotein structures were deduced from data presented here (Fig. 4 to 9) and elsewhere (15).

together, these data are consistent with the presence of a localized nucleosome over the *hsc82*-ΔHSE1 promoter. That this nucleosome is not stably positioned is indicated by the absence of chromatin-specific DNase I or MNase cleavages mapping to the mutated promoter region (Fig. 6 and 9A). This occluded nucleoprotein structure represents a dramatic contrast to the accessible, nucleosome-free state of the WT promoter, which is characterized by the presence of stably bound TBP (Fig. 5D). Structural models for the *HSC82*$^+$ and *hsc82*-ΔHSE1 upstream regions are provided in Fig. 10.

Notably, mutations in any one of four other regulatory elements upstream of *HSC82* have no comparable effect on promoter architecture. Indeed, HSE1 remains occupied and DNase I hypersensitivity remains essentially unaltered in *hsc82*

alleles bearing mutations in GRF2, URS1, HSE0, or TATA (Fig. 4 and 5; but see below). These results contrast with those of a recent study of the chicken β-globin gene enhancer, which found that hypersensitivity was determined by multiple factors which additively increased accessibility (9a). The findings reported here also extend previous observations suggesting that ScHSF is capable of binding nucleosomal DNA in vivo (24, 54), for they demonstrate that it can do so independently of other sequence-specific factors. This observation also provides a striking contrast to the behavior of *Drosophila* HSF, whose in vivo access to the *hsp70* promoter is critically dependent on DNA elements adjacent to the HSEs (58). In particular, displacement of nucleosomes by GAGA factor appears to be an essential prerequisite for HSF binding to *Drosophila* heat shock promoters (44, 46, 58). Similar remodeling of chromatin may be required for promoter occupancy by human HSF, given its inability to bind nucleosomal DNA in vitro (65), and *Xenopus* HSF, given its impaired ability to bind microinjected *hsp70* promoter DNA templates lacking Y-box elements (37). Importantly, our data do not rule out a role for global activators such as the SWI/SNF or NURF complexes (28, 31a, 55) in facilitating ScHSF-directed chromatin remodeling.

HSF stimulates transcription through its ability to alleviate nucleosomal repression. In addition to its dramatic impact on promoter architecture, the ΔHSE1 mutation essentially abolishes expression of the gene, reducing basal transcription 25-fold and induced transcription >100-fold (Table 2). Three lines of evidence argue that this inactivation is due to active nucleosomal repression. First, the TBP footprint is erased (Fig. 5D), suggesting that the occluding structure in *hsc82*-ΔHSE1 blocks TBP access to the promoter, thereby preventing efficient transcriptional initiation. Second, the GRF2 site remains strongly occupied (Fig. 4A), implying the presence of stably bound Grf2p (see below) within the mutant promoter. Third, it has been previously shown that a GRF2 site can function as a UAS in an episomal context (where chromatin may be less stable than seen here), activating transcription to an extent comparable to that of other weak activators (12). Thus, the nucleosome present within the *hsc82*-ΔHSE1 core promoter may block the ability of Grf2p, and other DNA-bound factors, to stimulate transcription. We conclude that HSF functions as an antirepressor at *HSC82*, antagonizing nucleosomal repression of both basal and induced transcription.

The stably bound TFIID complex limits core promoter accessibility. The twofold increase in *Taq*I cleavage at *hsc82*-ΔTATA (Fig. 7B) is intriguing and implies that the TFIID complex itself limits the accessibility of the promoter DNA to sequence-specific proteins. This is an unprecedented yet unsurprising observation, given the size of the yeast TFIID complex (56) and the proximity of the TATA box (position −98) to the *Taq*I site (position −140). Retention of an open promoter configuration at *hsc82*-ΔTATA argues against a significant structural role for the TATA box, consistent with comparable analyses of the *Drosophila hsp26* heat shock gene (45) and the yeast *HSP82*, *SUC2*, and *PHO5* genes (19, 28, 39).

GRF2 stabilizes in vivo protein-DNA interactions at HSE1 and TATA. Earlier mapping experiments suggested that the GRF2-binding protein (Grf2p/Reb1p) creates a nucleosome-free zone of ~230 bp within the UAS_G of *GAL1*, since deletion of the GRF2 site led to nucleosome encroachment over the mutated sequence (20). Stable occupancy of the GRF2 site in the *hsc82*-ΔHSE1 allele (Fig. 4A) argues that in contrast, Grf2p is incapable of preventing nucleosome formation over the *hsc82* core promoter. This is most clearly shown by the *Taq*I accessibility assay (Fig. 7A), which indicates that sequence within 60 bp of GRF2 is strongly occluded upon mutation of HSE1. Therefore, the ability of Grf2p ability to remodel chromatin structure appears to be context dependent. The alternative interpretation that a protein unrelated to Grf2p is actually bound to this site is unlikely for two reasons. First, the GRF2 element represents a perfect 8/8 match of conserved nucleotides to the Grf2p consensus (12, 41). Second, the pattern of guanine protection is virtually identical to that seen in an in vitro methylation interference assay with a related GRF2 site and partially purified Grf2p (11). Interestingly, the GRF2-binding factor may exert a mild repulsive effect on the adjacent upstream nucleosome, given that MNase cleavages are shifted ~20 bp downstream in the ΔGRF2 strain (Fig. 9B). A structural model of the *hsc82*-ΔGRF2 allele is presented in Fig. 10.

In addition to its mild effect on nucleosomal positioning, the GRF2 mutation affects protein-DNA interactions at other regulatory elements. The ΔGRF2 lesion weakens both enzymatic and chemical protection at HSE1 (Fig. 4A and 5A to C) and reduces DMS protection over the TATA box (Fig. 5D). These weakened interactions are not due to a fortuitous secondary mutation. Using genomic sequencing, we have confirmed the upstream sequence of the *hsc82*-ΔGRF2 allele between the URS1 and TATA elements (Fig. 5 and data not shown). Interestingly, mutation of either HSE1 or TATA has no detectable effect on GRF2 occupancy, arguing that such facilitation of binding is not reciprocal and therefore not reflective of true cooperativity. A very similar behavior has recently been described for the abundant DNA-binding protein RAP1, which appears to facilitate the in vivo binding of an adjacent activator at *TPI1* in a nonreciprocal fashion (13a). Also noteworthy is the fact that HSE1 occupancy at either $HSC82^+$ or *hsc82*-ΔGRF2 is largely unaffected by heat shock (Fig. 5C). This is unexpected, given the previously observed enhancement of HSF binding to *HSP82* accompanying heat shock (16, 23). While the basis for this difference is unclear, the presence of several functional HSEs at *HSP82* may facilitate cooperative interactions between induced HSF trimers that are not possible at *HSC82*.

How might the GRF2 factor facilitate the binding of HSF to chromatin? Given the abundance of Grf2p (1,000 to 2,000 molecules per diploid cell [12]) and the fact that its binding sites are found within a large number of polymerase II and polymerase III regulatory regions, we suggest that one of its roles is to destabilize local histone-DNA interactions until relatively scarce gene-specific factors such as HSF are available for binding. Such an activity may contribute to both expression and structural phenotypes of the ΔGRF2 mutation. For example, the attenuated TBP-TATA interaction might be a consequence of the destabilized HSF-HSE1 complex, as discussed above. We have previously demonstrated that one role for promoter-bound HSF is to stabilize the interaction of TBP with the core promoter of the closely related *HSP82* gene (24). Taken together with our previous results, the ΔGRF2 and ΔHSE1 phenotypes (Fig. 5D) provide compelling support for the notion that a critical physiological function of upstream activators is to increase recruitment of TBP to the promoter (13, 32, 33, 75).

Deletion of URS1 uncouples chromatin structure from gene activity. The absence of any detectable role for the URS1 element in regulating *HSC82* transcription (Fig. 3) is surprising, given its perfect match to the extended consensus (64) and its reported activity as either a mitotic repressor (52, 63) or a meiotic activator (9, 64). The absence of URS1 activity may therefore reflect an unfavorable sequence context (47), or it may be attributable to its uncharacteristic position within the *HSC82* promoter (upstream of the UAS), or both. A less

perfect but more favorably positioned URS1 motif is active as both a repressor and an HSE-dependent activator at *HSP82* (64). It is interesting that URS1 is more strongly occupied in the *hsc82*-ΔHSE1 allele than in *HSC82*$^+$ (Fig. 4A and data not shown), implying that stably bound HSF antagonizes the association of protein(s) with URS1.

Consistent with its negligible role in regulating transcription, URS1 exerts no effect on the nucleoprotein architecture of the *HSC82* core promoter. Interestingly, however, the sequence appears to actively participate in organizing the phasing frame of the upstream nucleosomal array. Specifically, the ΔURS1 mutation causes nucleosomes to shift at least 10 to 20 bp upstream, as well as become less precisely positioned with respect to the underlying DNA sequence. This phenotype, schematically depicted in Fig. 10, contrasts with that of the ΔGRF2 mutation, which is characterized by a translational shift toward the promoter. It would therefore appear that the combination of a weakly bound URS1 complex and tightly bound GRF2 factor (seen at both *HSC82*$^+$ and *hsc82*-ΔHSE1 alleles [Fig. 4A]) precisely positions the adjacent nucleosomal array, since mutation of one regulatory element or the other both shifts and diffuses its translational setting.

A central structural role for HSF in *S. cerevisiae*. In this study, we tested the hypothesis that *cis*-regulatory elements within the *HSC82* promoter regulate transcription, at least in part, through their ability to generate an accessible chromatin structure. As discussed above, only HSE1 mediates its effects through creation of an accessible, nucleosome-free promoter structure. This result, in conjunction with previous work demonstrating the ability of ScHSF to disrupt or displace nucleosomes at the *hsp82*-ΔHSE1 promoter (24), suggests that a critical physiological role of ScHSF is to remodel the chromatin structure of yeast core promoters. This function clearly contrasts with that played by the GRF2-binding protein, which cannot alleviate nucleosomal repression at either *hsc82*-ΔHSE1 or *GAL1*, despite its ability to constitutively bind DNA in vivo (Fig. 4A and data not shown). It is notable that GAL4, and not Grf2p, is required for disruption of the TATA-associated nucleosome during transcriptional induction of *GAL1* (6). The sharp contrast between GAL4 and ScHSF on the one hand and Grf2p on the other is intriguing and fortifies the notion that only a subset of transcription factors are capable of creating an accessible, nucleosome-free chromatin structure at the core promoter, site of formation of the preinitiation complex. We have previously suggested that proteins that are capable of reconfiguring nucleosomal structure be designated POWER (promoter open window entry regulator) factors (24). What distinguishes these POWER activators, such as ScHSF, GAL4, steroid hormone receptors, and GAGA factor (4, 6, 51, 67–69), from other sequence-specific activators, such as Grf2p, NF1, *Drosophila* HSF, and especially TBP (this study and references 4, 24, and 58), is an interesting and as yet unanswered question.

ACKNOWLEDGMENTS

A. M. Erkine and C. C. Adams contributed equally to this work.

We thank Mike Hampsey and Chris Szent-Gyorgyi for critical reading of the manuscript, Ned Sekinger and Kate Dayton for technical assistance, and Seewoo Lee, David Finkelstein, and Sue Lindquist for reagents.

This study was supported by grants from the National Institute of General Medical Sciences (GM45842) and the Center for Excellence in Cancer Research at LSUMC to D.S.G.

REFERENCES

1. **Adams, C. C., and D. S. Gross.** 1991. The yeast heat shock response is induced by the conversion of cells to spheroplasts and by potent transcriptional inhibitors. J. Bacteriol. **173:**7429–7435.
2. **Adams, C. C., and D. S. Gross.** Unpublished data.
3. **Almer, A., H. Rudolph, A. Hinnen, and W. Horz.** 1986. Removal of positioned nucleosomes from the yeast *PHO5* promoter upon *PHO5* induction releases additional upstream activating DNA elements. EMBO J. **5:**2689–2696.
4. **Archer, T. K., M. G. Cordingley, R. G. Wolford, and G. L. Hager.** 1991. Transcription factor access is mediated by accurately positioned nucleosomes on the mouse mammary tumor virus promoter. Mol. Cell. Biol. **11:**688–698.
5. **Ausubel, F. M., R. Brent, R. E. Kingston, D. D. Moore, J. G. Seidman, J. A. Smith, and K. Struhl (ed.).** 1995. Current protocols in molecular biology. John Wiley & Sons, Inc., New York.
6. **Axelrod, J. D., M. S. Reagan, and J. Majors.** 1993. GAL4 disrupts a repressing nucleosome during activation of *GAL1* transcription *in vivo*. Genes Dev. **7:**857–869.
7. **Becker, P. B., S. K. Rabindran, and C. Wu.** 1991. Heat shock-regulated transcription *in vitro* from a chromatin template. Proc. Natl. Acad. Sci. USA **88:**4109–4113.
8. **Borkovich, K. A., F. W. Farrelly, D. B. Finkelstein, J. Taulien, and S. Lindquist.** 1989. hsp82 is an essential protein that is required in higher concentrations for growth of cells at higher temperatures. Mol. Cell. Biol. **9:**3919–3930.
9. **Bowdish, K. S., H. E. Yuan, and A. P. Mitchell.** 1995. Positive control of yeast meiotic genes by the negative regulator *UME6*. Mol. Cell. Biol. **15:**2955–2961.
9a. **Boyes, J., and G. Felsenfeld.** 1996. Tissue-specific factors additively increase the probability of the all-or-none formation of a hypersensitive site. EMBO J. **15:**2496–2507.
10. **Buratowski, S.** 1994. The basics of basal transcription by RNA polymerase II. Cell **77:**1–3.
11. **Carmen, A. A., and M. J. Holland.** 1994. The upstream repression sequence from the yeast enolase gene *ENO1* is a complex regulatory element that binds multiple *trans*-acting factors including *REB1*. J. Biol. Chem. **269:**9790–9797.
12. **Chasman, D. I., N. F. Lue, A. R. Buchman, J. W. LaPointe, Y. Lorch, and R. D. Kornberg.** 1990. A yeast protein that influences the chromatin structure of UAS_G and functions as a powerful auxiliary gene activator. Genes Dev. **4:**503–514.
13. **Chatterjee, S., and K. Struhl.** 1995. Connecting a promoter-bound protein to TBP bypasses the need for a transcriptional activation domain. Nature (London) **374:**820–822.
13a. **Drazinic, C. M., J. B. Smerage, M. C. Lopez, and H. V. Baker.** 1996. Activation mechanism of the multifunctional transcription factor repressor-activator protein 1 (Rap1p). Mol. Cell. Biol. **16:**3187–3196.
14. **Elgin, S. C. R.** 1988. The formation and function of DNase hypersensitive sites in the process of gene activation. J. Biol. Chem. **263:**19259–19262.
15. **Erkine, A. M., C. C. Adams, M. Gao, and D. S. Gross.** 1995. Multiple protein-DNA interactions over the yeast *HSC82* heat shock gene promoter. Nucleic Acids Res. **23:**1822–1829.
16. **Erkine, A. M., and D. S. Gross.** Unpublished data.
17. **Erkine, A. M., C. Szent-Gyorgyi, S. F. Simmons, and D. S. Gross.** 1995. The upstream sequences of the *HSP82* and *HSC82* genes of *Saccharomyces cerevisiae*: regulatory elements and nucleosome positioning motifs. Yeast **11:**573–580.
18. **Fascher, K.-D., J. Schmitz, and W. Horz.** 1990. Role of *trans*-activating proteins in the generation of active chromatin at the *PHO5* promoter in *S. cerevisiae*. EMBO J. **9:**2523–2528.
19. **Fascher, K.-D., J. Schmitz, and W. Horz.** 1993. Structural and functional requirements for the chromatin transition at the *PHO5* promoter in *Saccharomyces cerevisiae* upon *PHO5* activation. J. Mol. Biol. **231:**658–667.
20. **Fedor, M. J., N. F. Lue, and R. D. Kornberg.** 1988. Statistical positioning of nucleosomes by specific protein-binding to an upstream activating sequence in yeast. J. Mol. Biol. **204:**109–127.
21. **Felsenfeld, G.** 1992. Chromatin as an essential part of the transcriptional mechanism. Nature (London) **355:**219–224.
22. **Fernandes, M., H. Xiao, and J. T. Lis.** 1994. Fine structure analyses of the *Drosophila* and *Saccharomyces* heat shock factor-heat shock element interactions. Nucleic Acids Res. **22:**167–173.
22a. **Fernandes, M., H. Xiao, and J. T. Lis.** 1995. Binding of heat shock factor to and transcriptional activation of heat shock genes in *Drosophila*. Nucleic Acids Res. **23:**4799–4804.
23. **Giardina, C., and J. T. Lis.** 1995. Dynamic protein-DNA architecture of a yeast heat shock promoter. Mol. Cell. Biol. **15:**2737–2744.
23a. **Goodson, M. L., and K. D. Sarge.** 1995. Heat-inducible DNA binding of purified heat shock transcription factor 1. J. Biol. Chem. **270:**2447–2450.
24. **Gross, D. S., C. C. Adams, S. Lee, and B. Stentz.** 1993. A critical role for heat shock transcription factor in establishing a nucleosome-free region over the TATA-initiation site of the yeast *HSP82* heat shock gene. EMBO J. **12:**3931–3945.
25. **Gross, D. S., K. E. English, K. W. Collins, and S. Lee.** 1990. Genomic footprinting of the yeast *HSP82* promoter reveals marked distortion of the

DNA helix and constitutive occupancy of heat shock and TATA elements. J. Mol. Biol. **216:**611–631.
26. **Gross, D. S., and W. T. Garrard.** 1988. Nuclease hypersensitive sites in chromatin. Annu. Rev. Biochem. **57:**159–197.
27. **Grunstein, M.** 1990. Histone function in transcription. Annu. Rev. Cell Biol. **6:**643–678.
28. **Hirschhorn, J. N., S. A. Brown, C. D. Clark, and F. Winston.** 1992. Evidence that SNF2/SWI2 and SNF5 activate transcription in yeast by altering chromatin structure. Genes Dev. **6:**2288–2298.
29. **Jakobsen, B. K., and H. R. B. Pelham.** 1988. Constitutive binding of yeast heat shock factor to DNA in vivo. Mol. Cell. Biol. **8:**5040–5042.
30. **Jenuwein, T., W. C. Forrester, R.-G. Qiu, and R. F. Grosschedl.** 1993. The immunoglobulin μ enhancer core establishes local factor access in nuclear chromatin independent of transcriptional stimulation. Genes Dev. **7:**2016–2032.
31. **Kim, J. L., D. B. Nikolov, and S. K. Burley.** 1993. Co-crystal structure of TBP recognizing the minor groove of a TATA element. Nature (London) **365:** 520–527.
31a. **Kingston, R. E., C. A. Bunker, and A. N. Imbalzano.** 1996. Repression and activation by multiprotein complexes that alter chromatin structure. Genes Dev. **10:**905–920.
32. **Klages, N., and M. Strubin.** 1995. Stimulation of RNA polymerase II transcription initiation by recruitment of TBP *in vivo*. Nature (London) **374:**822–823.
33. **Klein, C., and K. Struhl.** 1994. Increased recruitment of TATA-binding protein to the promoter by transcriptional activation domains *in vivo*. Science **266:**280–282.
34. **Knezetic, J. A., and D. S. Luce.** 1986. The presence of nucleosomes on a DNA template prevents initiation by RNA polymerase II *in vitro*. Cell **45:** 95–101.
35. **Kornberg, R. D., and Y. Lorch.** 1991. Irresistible force meets immovable object: transcription and the nucleosome. Cell **67:**833–836.
36. **Kurtz, S., J. Rossi, L. Petko, and S. Lindquist.** 1986. An ancient developmental induction: heat shock proteins induced in sporulation and oogenesis. Science **231:**1154–1157.
37. **Landsberger, N., and A. P. Wolffe.** 1995. Role of chromatin and *Xenopus laevis* heat shock transcription factor in regulation of transcription from the *X. laevis hsp70* promoter in vivo. Mol. Cell. Biol. **15:**6013–6024.
38. **Laybourn, P. J., and J. T. Kadonaga.** 1991. Role of nucleosome cores and histone H1 in regulation of transcription by RNA polymerase II. Science **254:**238–245.
39. **Lee, M. S., and W. T. Garrard.** 1992. Uncoupling gene activity from chromatin structure: promoter mutations can inactivate transcription of the yeast *HSP82* gene without elimination of nucleosome-free regions. Proc. Natl. Acad. Sci. USA **89:**9166–9170.
40. **Lee, S., and D. S. Gross.** 1993. Conditional silencing: the *HMRE* mating-type silencer exerts a rapidly reversible position effect on the yeast *HSP82* heat shock gene. Mol. Cell. Biol. **13:**727–738.
41. **Liaw, P. C., and C. J. Brandl.** 1994. Defining the sequence specificity of *Saccharomyces cerevisiae* DNA binding protein Reb1p by selecting random-sequence oligonucleotides. Yeast **10:**771–787.
42. **Lis, J., and C. Wu.** 1993. Protein traffic on the heat shock promoter: parking, stalling, and trucking along. Cell **74:**1–4.
43. **Lorch, Y., J. W. LaPointe, and R. D. Kornberg.** 1987. Nucleosomes inhibit the initiation of transcription but allow chain elongation with the displacement of histones. Cell **49:**203–210.
44. **Lu, Q., L. L. Wallrath, B. D. Allan, R. L. Glaser, J. T. Lis, and S. C. R. Elgin.** 1992. Promoter sequence containing $(CT)_n \cdot (GA)_n$ repeats is critical for the formation of the DNase I hypersensitive sites in the *Drosophila hsp26* gene. J. Mol. Biol. **225:**985–998.
45. **Lu, Q., L. L. Wallrath, P. A. Emanuel, S. C. R. Elgin, and D. S. Gilmour.** 1994. Insensitivity of the preset *hsp26* chromatin structure to a TATA box mutation in *Drosophila*. J. Biol. Chem. **269:**15906–15911.
46. **Lu, Q., L. L. Wallrath, H. Granok, and S. C. R. Elgin.** 1993. $(CT)_n \cdot (GA)_n$ repeats and heat shock elements have distinct roles in chromatin structure and transcriptional activation of the *Drosophila hsp26* gene. Mol. Cell. Biol. **13:**2802–2814.
47. **Luche, R. M., R. Sumadra, and T. G. Cooper.** 1990. A *cis*-acting element present in multiple genes serves as a repressor protein binding site for the yeast *CAR1* gene. Mol. Cell. Biol. **10:**3884–3895.
48. **McDaniel, D., A. J. Caplan, M. S. Lee, C. C. Adams, B. R. Fishel, D. S. Gross, and W. T. Garrard.** 1989. Basal-level expression of the yeast *HSP82* gene requires a heat shock regulatory element. Mol. Cell. Biol. **9:**4789–4798.
49. **Mitchell, A. P.** 1994. Control of meiotic gene expression in *Saccharomyces cerevisiae*. Microbiol. Rev. **58:**56–70.
50. **Morrow, B. E., Q. Ju, and J. R. Warner.** 1993. A bipartite DNA-binding domain in yeast Reb1p. Mol. Cell. Biol. **13:**1173–1182.
51. **Morse, R. H.** 1993. Nucleosome disruption by transcription factor binding in yeast. Science **262:**1563–1566.
52. **Park, H.-O., and E. A. Craig.** 1989. Positive and negative regulation of basal expression of a yeast *HSP70* gene. Mol. Cell. Biol. **9:**2025–2033.
53. **Pazin, M. J., R. T. Kamakaka, and J. T. Kadonaga.** 1994. ATP-dependent nucleosome reconfiguration and transcriptional activation from preassembled chromatin templates. Science **266:**2007–2011.
54. **Pederson, D. S., and T. Fidrych.** 1994. Heat shock factor can activate transcription while bound to nucleosomal DNA in *Saccharomyces cerevisiae*. Mol. Cell. Biol. **14:**189–199.
55. **Peterson, C. L., and J. W. Tamkun.** 1995. The SWI-SNF complex: a chromatin remodeling machine? Trends Biochem. Sci. **20:**143–146.
56. **Poon, D., Y. Bai, A. M. Campbell, S. Bjorklund, Y.-J. Kim, S. Zhou, R. D. Kornberg, and P. A. Weil.** 1995. Identification and characterization of a TFIID-like multiprotein complex from *Saccharomyces cerevisiae*. Proc. Natl. Acad. Sci. USA **92:**8224–8228.
57. **Prioleau, M., J. Huet, A. Sentenac, and M. Mechali.** 1994. Competition between chromatin and transcription complex assembly regulates gene expression during early development. Cell **77:**439–449.
58. **Shopland, L. S., K. Hirayoshi, M. Fernandes, and J. T. Lis.** 1995. HSF access to heat shock elements *in vivo* depends critically on promoter architecture defined by GAGA factor, TFIID, and RNA polymerase II binding sites. Genes Dev. **9:**2756–2769.
59. **Sikorski, R., and P. Hieter.** 1989. A system of shuttle vectors and yeast host strains designed for efficient manipulation of DNA in *Saccharomyces cerevisiae*. Genetics **122:**19–27.
60. **Sorger, P. K., M. J. Lewis, and H. R. B. Pelham.** 1987. Heat shock factor is regulated differently in yeast and HeLa cells. Nature (London) **329:**81–84.
61. **Sorger, P. K., and H. C. M. Nelson.** 1989. Trimerization of a yeast transcriptional activator via a coiled-coil motif. Cell **59:**807–813.
62. **Straka, C., and W. Horz.** 1991. A functional role for nucleosomes in the repression of a yeast promoter. EMBO J. **10:**361–368.
63. **Sumrada, R. A., and T. G. Cooper.** 1987. Ubiquitous upstream repression sequences control activation of the inducible arginase gene in yeast. Proc. Natl. Acad. Sci. USA **84:**3997–4001.
64. **Szent-Gyorgyi, C.** 1995. A bipartite operator interacts with a heat shock element to mediate early meiotic induction of *Saccharomyces cerevisiae HSP82*. Mol. Cell. Biol. **15:**6754–6769.
65. **Taylor, I. C., J. L. Workman, T. J. Schuetz, and R. E. Kingston.** 1991. Facilitated binding of GAL4 and heat shock factor to nucleosomal templates: differential function of DNA-binding domains. Genes Dev. **5:**1285–1298.
66. **Tjian, R., and T. Maniatis.** 1994. Transcriptional activation: a complex puzzle with few easy pieces. Cell **77:**5–8.
67. **Truss, M., J. Bartsch, A. Schelbert, R. J. G. Hache, and M. Beato.** 1995. Hormone induces binding of receptors and transcription factors to a rearranged nucleosome on the MMTV promoter *in vivo*. EMBO J. **14:**1737–1751.
68. **Tsukiyama, T., P. B. Becker, and C. Wu.** 1994. ATP-dependent nucleosome disruption at a heat-shock promoter mediated by binding of GAGA transcription factor. Nature (London) **367:**525–532.
69. **Wall, G., P. D. Varga-Weisz, R. Sandaltzopoulos, and P. B. Becker.** 1995. Chromatin remodeling by GAGA factor and heat shock factor at the hypersensitive *Drosophila hsp26* promoter *in vitro*. EMBO J. **14:**1727–1736.
70. **Werner-Washburne, M., J. Becker, J. Kosic-Smithers, and E. A. Craig.** 1989. Yeast Hsp70 RNA levels vary in response to the physiological status of the cell. J. Bacteriol. **171:**2680–2688.
71. **Wolffe, A. P.** 1994. Transcription: in tune with the histones. Cell **77:**13–16.
72. **Workman, J. L., and A. R. Buchman.** 1993. Multiple functions of nucleosomes and regulatory factors in transcription. Trends Biochem. Sci. **18:**90–95.
73. **Workman, J. L., and R. G. Roeder.** 1987. Binding of transcription factor TFIID to the major late promoter during *in vitro* nucleosome assembly potentiates subsequent initiation by RNA polymerase II. Cell **51:**613–622.
74. **Workman, J. L., R. G. Roeder, and R. E. Kingston.** 1990. An upstream transcription factor, USF (MLTF), facilitates the formation of preinitiation complexes during *in vitro* chromatin assembly. EMBO J. **9:**1299–1308.
75. **Xiao, H., J. D. Friesen, and J. T. Lis.** 1995. Recruiting TATA-binding protein to a promoter: transcriptional activation without an upstream activator. Mol. Cell. Biol. **15:**5757–5761.